New Galactic embedded clusters and candidates from a WISE Survey

D. Camargo, E. Bica, C. Bonatto

Departamento de Astronomia, Universidade Federal do Rio Grande do Sul, Av. Bento Gonçalves 9500 Porto Alegre 91501-970, RS, Brazil

arXiv:1406.3099v2 [astro-ph.SR] 24 Jun 2014

Abstract

We carried out a search for new infrared star clusters, stellar groups and candidates using WISE images, which are very sensitive to dust emission nebulae. We report the discovery of 437 embedded clusters and stellar groups that show a variety of structures, both in the stellar and nebular components. Pairs or small groupings of clusters are observed, suggesting multiple generations at the early formation stages. The resulting catalogue provides Galactic and equatorial coordinates, together with angular sizes for all objects. The nature of a representative test sub-sample of 14 clusters is investigated in detail by means of 2MASS photometry. The colour magnitude diagrams and radial density distributions characterize them as stellar clusters. The 437 new objects were found in the ranges $145^\circ \leq \ell \leq 290^\circ$ and $-25^\circ \leq b \leq 20^\circ$, and they appear to be a major object source for future studies of star cluster formation and their early evolution. WISE is a powerful tool to further probe for very young clusters throughout the disk.

Keywords: open clusters and associations

1. Introduction

Dust enshrouded star clusters have been systematically studied with relatively large samples in the near infrared since Hodapp (1994), as detectors became efficient enough. In the early 2000's several lists of new dusty clusters were provided (Ivanov et al., 2002; Bica et al., 2003a; Dutra et al., 2003). At that time efforts were made to compile catalogues of this object class (Lada & Lada, 2003; Bica et al., 2003b). Some young clusters have been studied in X-rays with Chandra (e.g. Ybarra et al., 2013). Recently, Majaess (2013) used WISE together with other data to discover 229 new dust related stellar clusters. The latter findings involving WISE near and mid infrared bands indicate the importance to carry out new searches for stellar clusters in formation and early evolutionary stages.

The Galaxy appears to contain $\sim 10^5$ open clusters (Bonatto et al., 2006; Piskunov et al., 2006) but only ~ 2000 have astrophysical parameters determined (DAML02[1], WEBDA[2]). The completeness effects in the OC system are due mainly to the higher extinction and stellar crowding in the disc (Lada et al., 1991; Hodapp, 1994; Bica et al., 2003b).

Stellar clusters are fundamental tools to improve our understanding of the Galactic structure, star formation history, and evolution (Friel, 1995; Bonatto et al., 2006; Piskunov et al., 2006; Bobylev, 2007; Camargo, Bica & Bonatto, 2013; Bobylev & Bajkova, 2014). Most star formation occurs in crowded environments, such as in embedded clusters (ECs) and embedded stellar groups. ECs are formed in giant molecular clouds (GMCs), in dense clumps with size of ~ 1 pc. Since ECs can be heavily obscured , most of them are detected in the infrared. The development of infrared array detectors in recent decades has boosted our knowledge of these objects. As a result sky surveys provided new objects (Dutra et al., 2003; Bica et al., 2003a,b; Bica & Bonatto, 2005; Kharchenko et al., 2005a,b; Mercer et al., 2005; Kronberger et al., 2006; Froebrich, Scholz & Raftery, 2007; Koposov et al., 2008; Glushkova et al., 2010; Borissova et al., 2011). Recently, we discovered 16 new ECs (CBB 1 - CBB 16), some of them within groups of clusters (Camargo, Bonatto & Bica, 2011, 2012; Camargo, Bica & Bonatto, 2013). A fundamental contribution of such detailed studies of individual clusters is homogenously derived astrophysical parameters.

Most (if not all) stars form in star clusters (Lada et al., 1991; Hodapp, 1994; Lada & Lada, 2003). In this sense, they are frequently considered as the building blocks in galaxy construction. Lada & Lada (2003) define a cluster as a group of physically related stars that survive longer than 100 Myr as a bound system. This requires at least 35 stars and stellar-mass density larger than $1 M_\odot / pc^{-3}$. Adams & Myers (2001) indicate three ways to form stars: isolated singles and binaries, stellar groups (10 to 100 members), and clusters (> 100 stars). They argue that stellar groups are the most common way to form stars. Hodapp (1994) considers cluster the stellar groups with five or more stars.

In this paper we carry out a search for new embedded

[1] http://www.astro.iag.usp.br/ wilton/ (Dias et al., 2002).
[2] http://obswww.unige.ch/webda (Mermelliod, 1996).

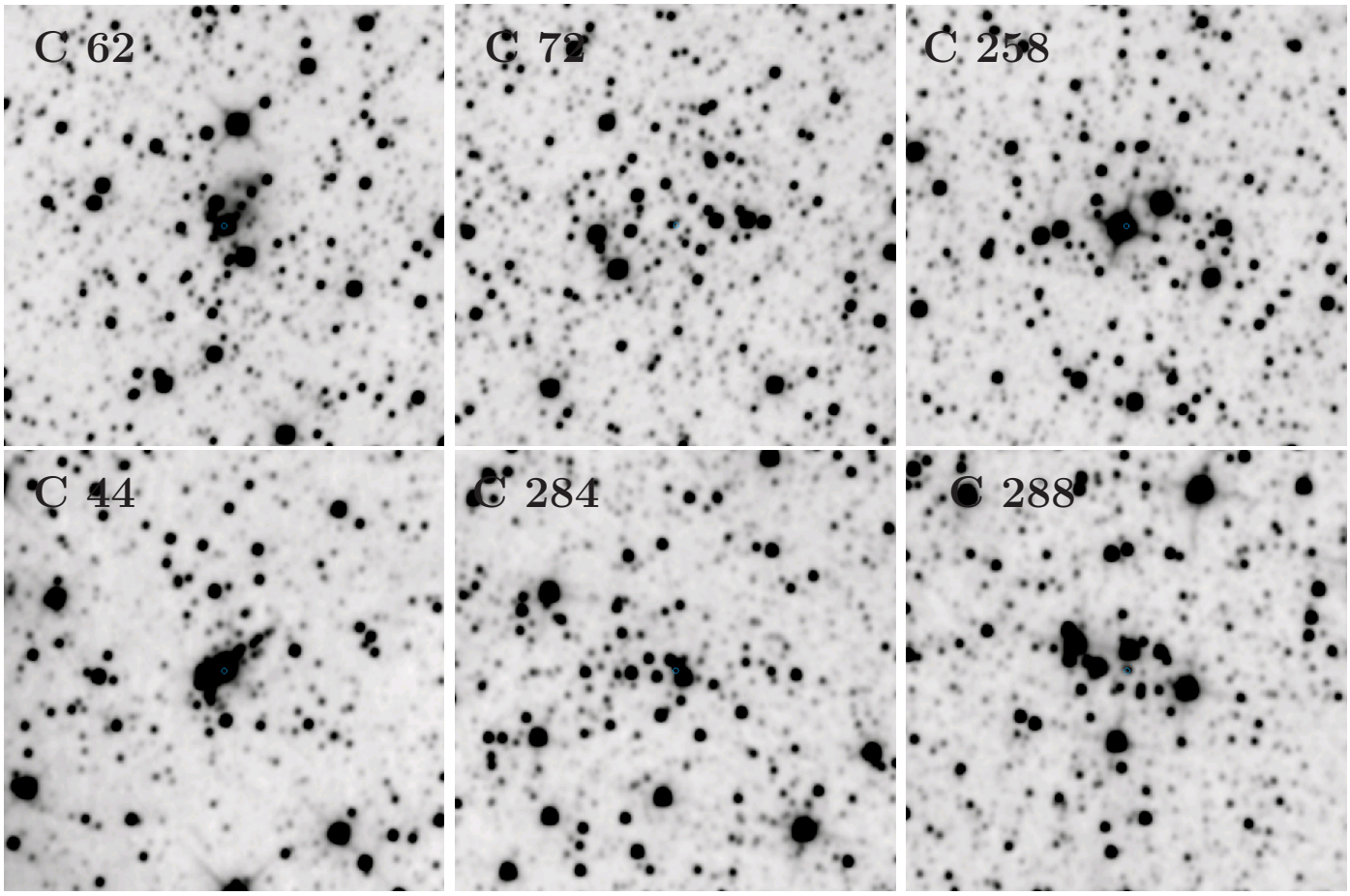

Figure 1 Examples of sample clusters. Top panels: W1 WISE images ($10' \times 10'$) centred on C 62, C 72, and C 258. Bottom: W2 images centred on C 44, C 284, and C 288. These objects are classified as ECs.

clusters using WISE band images. We were encouraged by the impressive large number of recent discoveries by Majaess (2013). However, we employ a complementary different method.

This paper is organized as follows. In Sect. 2 we present the new clusters found in this study. In Sect. 3 we discuss the stellar density and dust distributions. In Sect. 3 we highlight star formation stages that are possibly related to the dust distribution, and in turn infer forming processes themselves. In Sect. 4 we employ 2MASS photometry for a selection of 14 new clusters to test their reality. In Sect. 5 we analyse the corresponding CMDs and RDPs. Finally, in Sect. 6 we give the concluding remarks.

2. New star clusters and candidates

We searched for new clusters, stellar groups, and candidates in the WISE[3] (Wright et al., 2010) image atlas. WISE is a survey covering the entire sky in the infrared bands W1, W2, W3, and W4 centred at 3.4, 4.6, 12 and 22μm. The project was funded by NASA and operated by the Jet Propulsion Laboratory (JPL). The data processing and analysis was done by the Infrared Processing and Analysis Center (IPAC). Processed images and data are online available via NASA/IPAC Infrared Science Archive (IRSA).

WISE provides very efficient detections of star forming clusters (Majaess, 2013). We searched for new clusters, stellar groups and candidates in dust nebulae in the 3rd Quadrant and extensions to the 2nd and 4th Quadrants (Table 1). WISE images for a representative sample of the newly found clusters are shown in Figs. 1 to 6.

Recently, Majaess (2013) employed WISE in a search for very young clusters. His method differs from the present one in the sense that he employs a hybrid $JHK_s - W_1W_2W_3W_4$ photometry to identify concentrations of young stellar objects (YSOs). Our search focuses on the stellar density and gas/dust distribution to identify star clusters, stellar groups, and candidates. A similar early procedure was used by Hodapp (1994) who analysed 164 nebulae with molecular outflow sources, 54 of them resulting associated with embedded clusters. Also similarly, Bica et al. (2003a) and Dutra et al. (2003), in a survey around the Galactic disk, provided 346 infrared clusters,

[3]The Wide-field Infrared Survey Explorer

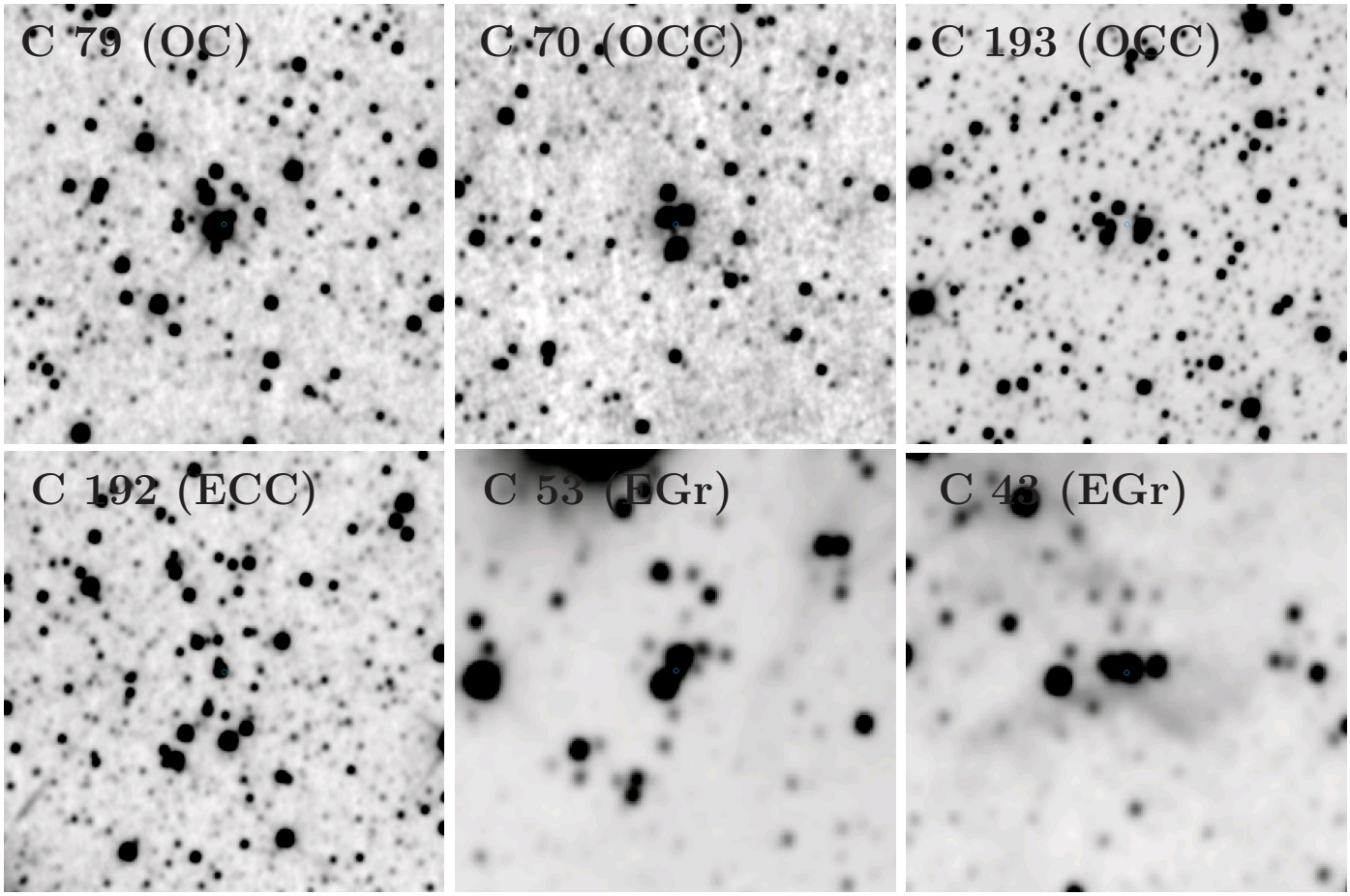

Figure 2 Examples of additional sample classifications. Top panels: W2 WISE images ($10' \times 10'$) centred on the OC C 79 and on the OCCs C 70, and C 193. Bottom: W2 images ($10' \times 10'$) centred on the ECC C 192 and W2 images ($5' \times 5'$) centred on the EGrs C 53, and C 43.

stellar groups, and candidates.

The object search started with inspection of $2° \times 2°$ WISE images near the Galactic plane. We used the WISE standard RGB colour images primarily looking for dust emission nebulae at different temperatures in the wavelength bands W1, W2, W3, and W4. Subsequently, we were guided by stellar concentrations.

The survey provided 437 new star clusters, stellar groups, and candidates. The discovered objects were classified in five classes: open clusters (OCs), open cluster candidates (OCCs), embedded clusters (ECs), embedded cluster candidates (ECCs), and embedded stellar groups (EGrs). The classification follows a stellar/dust density estimation on the W1, W2, W3, W4, and RGB WISE images. Populous dust-free objects are classified as OCs and the OCCs are in general poor or unresolved objects that require deeper photometry or higher resolution. Prominent objects that are still cradled in their natal molecular clouds are ECs and the less populous candidates are ECCs. Star-forming low density groups are EGrs. Fig. 1 shows a representative sample of ECs and Fig. 2 shows samples of OC, OCC, ECC, and EGr.

Table 1 The new list of star clusters or candidates.

Target	ℓ	b	α(2000)	δ(2000)	Size	Type	Avend.
	(°)	(°)	(h m s)	(° ′ ″)	(′)		
(1)	(2)	(3)	(4)	(5)	(6)	(7)	(8)
C 1	147.52	10.03	4:44:32	61:12:03	8 × 8	EC	n
C 2	147.88	9.46	4:42:50	60:33:46	9 × 9	EC	n
C 3	147.99	9.79	4:45:28	60:41:25	10 × 10	EC	n
C 4	149.83	-24.50	2:47:55	32:13:07	8 × 8	OCC	n
C 5	151.83	15.69	5:42:49	60:51:31	7 × 7	EC	n
C 6	151.84	16.06	5:45:34	61:01:36	8 × 8	EC	n
C 7	151.96	16.11	5:46:19	60:56:45	12 × 12	ECC	n
C 8	151.97	15.52	5:42:05	60:39:31	5 × 5	EC	n
C 9	152.12	16.14	5:47:08	60:49:12	6 × 6	EGr	n
C 10	152.30	15.76	5:45:02	60:29:36	6 × 6	EGr	n
C 11	160.11	-18.43	3:41:22	31:54:37	4 × 4	EC	n
C 12	160.28	-18.42	3:41:58	31:48:45	6 × 6	EC	n
C 13	164.15	0.56	5:03:50	42:22:15	5 × 5	EC	n
C 14	169.52	-1.79	5:10:50	36:39:45	6 × 6	EC	n
C 15	170.13	-1.17	5:15:04	36:31:54	7 × 7	EGr	n
C 16	171.17	0.45	5:24:41	36:36:16	5 × 5	EC	y
C 17	171.43	-0.01	5:23:30	36:07:49	7 × 7	EC	n
C 18	171.77	1.45	5:30:30	36:39:53	7 × 7	EC	n
C 19	172.08	-2.26	5:16:18	34:18:54	4 × 4	EGr	y
C 20	172.42	2.44	5:36:23	36:39:41	5 × 5	EC	n

Table Notes. We suggest the designation Camargo for the objects, since one of us (D.C.) discovered them. Cols. 2 – 5: Central coordinates. Col. 6: cluster size. Col. 7: object type - OC means open cluster, OCC open cluster candidate, EC embedded cluster, ECC embedded cluster candidate, and EGr stellar group. Col. 8: cross-identifications with Avedisova (2002) SFRs or candidates within 5' of the central coordinates, y and n means yes and not. The full table is available online.

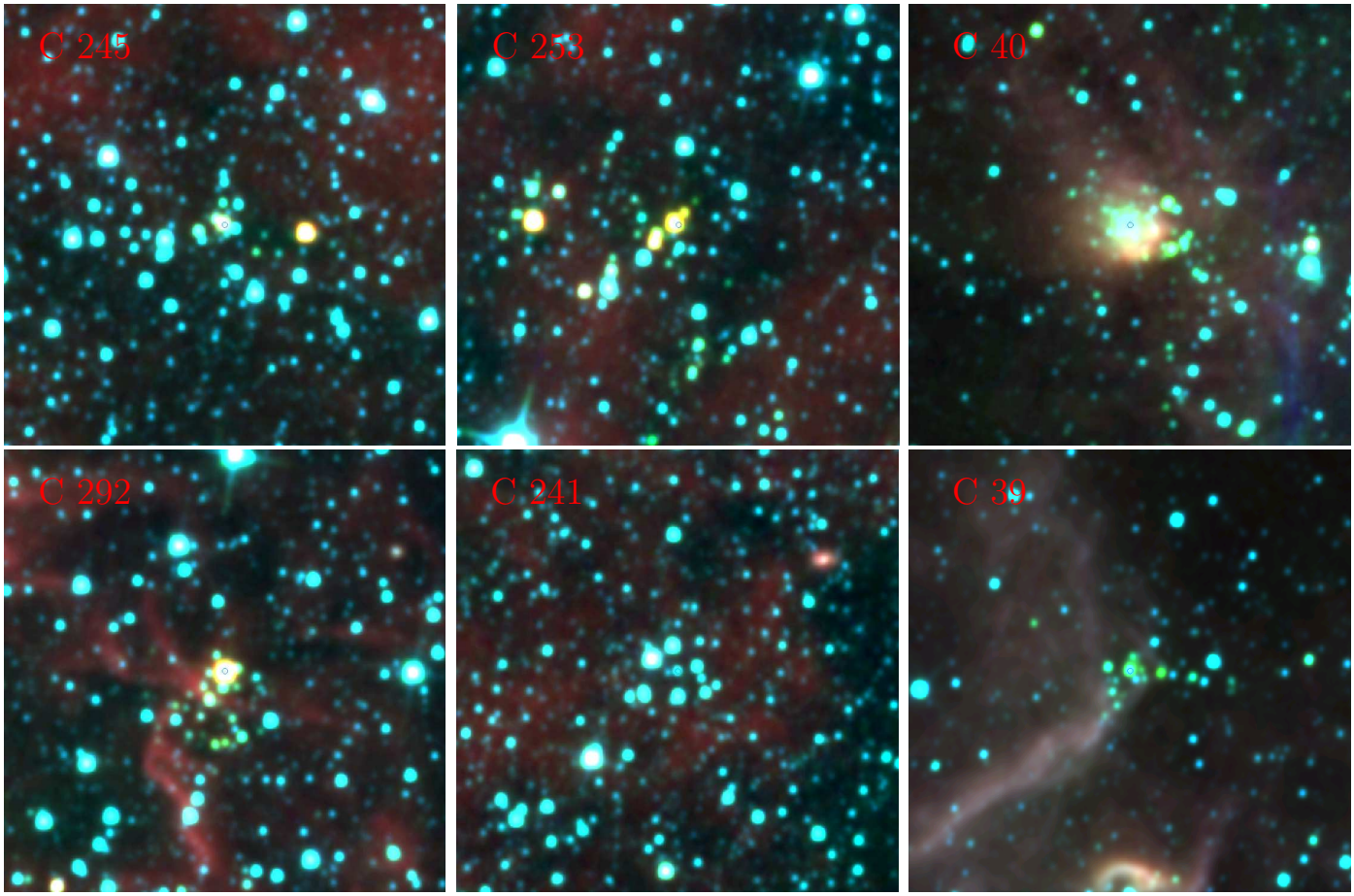

Figure 3 RGB examples of various cluster/dust distributions in sample objects. Top panels: WISE RGB images ($10' \times 10'$) centred on C 245, C 253 and C 40. Bottom panels: the same for C 292, C 241, and C 39. C 292 is in the central region of a bubble. These objects are ECs.

We verified that the present objects do not have previous identifications in the literature. The comparison catalogue that we used is essentially complete for all published star clusters in the Galaxy and was made by one of us, E.B., and will be presented in a forthcoming paper. Additionally, we used e.g. SIMBAD, the catalogue of infrared star clusters, stellar groups and candidates by Bica et al. (2003a), the cluster and candidate catalogue by Froebrich, Scholz & Raftery (2007), the recent protocluster results in WISE by Majaess (2013), and many others. We also cross correlated our cluster dust emission nebulae with the planetary nebulae catalogue of Acker et al. (1992). This way we could also classify some clump candidates as probable star-forming nebulae (SFNs) in the present list Table 1.

During our WISE search for stellar clusters and candidates, we came across with 49 objects from the literature (Table 2). They belong mostly to our EC classification, except the OC NGC 2301, and the OCCs FSR 1144 and FSR 1149. The FSR object recognition as ECs was derived by us from the WISE images. This cross-identification effort is important to cross relate classifications in other lists, catalogues and individual papers.

Avedisova (2002) presented 3300 star forming regions (SFRs), of which about 500 are candidates. She complemented this with available photometric data and presented information on diffuse and reflecting nebulae, dark and molecular clouds. Her data do not refer directly to star clusters. It is fundamental to cross-identify her results with ours found in the WISE bands, in view of establishing or not the presence of stellar clusters. These comparisons might help answer questions such as *i*) are very young clusters systematically found outside or inside Avendisova's SFRs? *ii*) Clues about the threshold of cluster/individual star formation? The cross-identifications within 5' of the central coordinates provided 95 coincidences between Avedisova (2002) and the present list of 437 entries. This amounts to 21.7% of our sample. We indicate in Table 1 the entries that coincided with Avendisova ones.

Out of the 437 objects, 297 ($\sim$ 67.9%) were classified as ECs, 23 ($\sim$ 5.3%) are ECCs, 90 ($\sim$ 20.8%) are EGrs, and the remaining 27 ($\sim$ 6.2%) are OCCs. These classes may suffer from completeness effects, especially the less dense

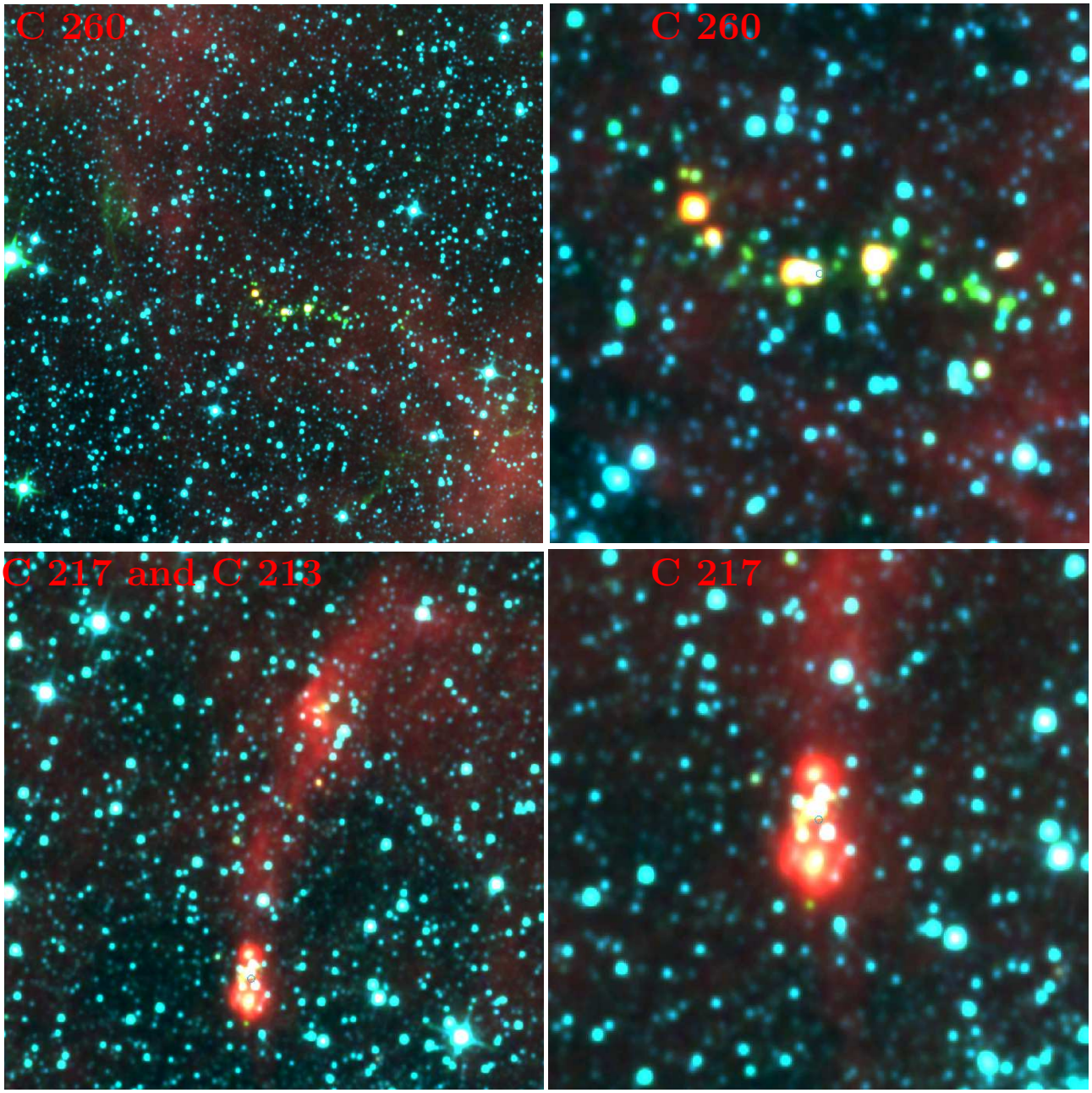

Figure 4 Cluster in filamentary dust structures. Top panels: WISE RGB images centred on C 260 ($40' \times 40'$), and C 260 ($10' \times 10'$). Bottom panels: the same for C 217 and C 213 ($30' \times 30'$), and C 217 ($10' \times 10'$). These images show evidence of filamentary cluster formation. C 260 shows unusual s-shaped structure.

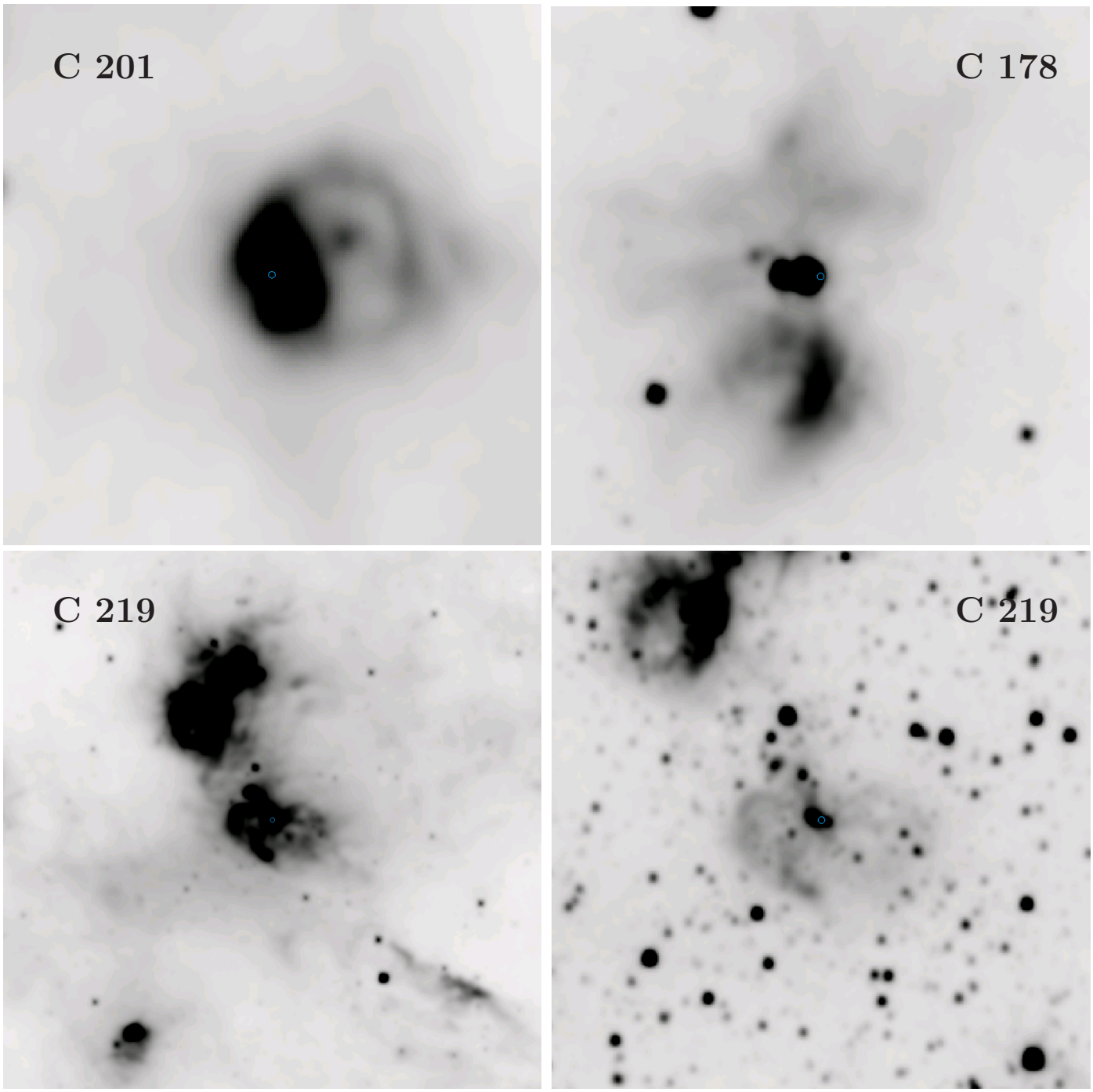

Figure 5 Examples of objects with remarkable structure in the sample. Top panels: W3 WISE images centred on C 201 ($5' \times 5'$), and C 178 ($10' \times 10'$). Bottom panels: the W3 WISE image for C 219 ($20' \times 20'$) and W2 WISE image for C 219 ($10' \times 10'$).

Table 2 Objects from the literature detected during our WISE search.

ℓ (°)	b (°)	α(2000) (h m s)	δ(2000) (° ′ ″)	Diameter (′)	Type	Designation	Reference
160.48	-17.81	3:44:33	32:09:19	10	EC	IC 348	Lada & Lada (2003)
169.93	-0.60	5:16:49	37:01:16	7	EC	Majaess 54	Majaess (2013)
170.66	-0.27	5:20:16	36:37:21	6	EC	KKC 6	Kumar et al. (2006)
170.72	-0.11	5:21:07	36:39:45	7	EC	Majaess 56	Majaess (2013)
170.82	0.01	5:21:53	36:38:52	5	EC	Majaess 57	Majaess (2013)
171.87	0.45	5:26:37	36:01:46	8	EC	Czernik 21	Maciejewski & Niedzielski (2007)
173.08	-3.46	5:14:22	32:48:13	7	EC	Dolidze 16	Camargo, Bonatto & Bica (2010)
195.62	-2.91	6:08:32	13:58:09	8	EC	NGC 2169	Krone-Martins et al. (2010)
211.88	-1.32	6:44:49	0:20:18	6	EC	PHN 2	Puga et al. (2009)
212.27	-1.08	6:46:22	0:04:46	7	EC	PHN 3	Puga et al. (2009)
212.54	0.28	6:51:46	0:28:21	11	OC	NGC 2301	Sharma et al. (2006)
214.07	-19.65	5:42:49	-9:47:22	10	EC	Majaess 64	Majaess (2013)
216.84	0.81	7:01:27	-3:06:41	4.5	EC	de Wit 2	de Wit et al. (2004)
217.49	-0.02	6:59:43	-4:04:00	3	EC	Ivanov 9	Ivanov et al. (2002)
217.63	-0.18	6:59:24	-4:15:54	4	EC	BDS 89	Bica et al. (2003b)
218.15	-0.64	6:58:41	-4:56:13	5	EC	FSR 1129	Froebrich, Scholz & Raftery (2007)
219.47	-10.57	6:25:14	-10:33:32	5	EC	BDS 91	Bica et al. (2003b)
219.49	-1.72	6:57:15	-6:37:12	10	OCC	FSR 1144	Froebrich, Scholz & Raftery (2007)
220.07	-0.11	7:04:06	-6:24:02	10	OCC	FSR 1149	Froebrich, Scholz & Raftery (2007)
220.79	-1.71	6:59:42	-7:46:29	5	EC	NGC 2316	Hodapp (1994)
224.01	-1.81	7:05:16	-10:40:10	5	EC	FSR 1178	Froebrich, Scholz & Raftery (2007)
224.23	-1.47	7:06:56	-10:43:45	7	EC	Collinder 466	Bukowiecki et al. (2011)
224.44	-2.36	7:04:08	-11:18:58	4	EC	Soares-Bica 1	Soares & Bica (2002)
224.40	-2.73	7:02:42	-11:27:03	5	EC	FSR 1184	Froebrich, Scholz & Raftery (2007)
224.50	-2.41	7:04:03	-11:23:40	4	EC	BRC 27	Soares & Bica (2002)
224.79	-1.73	7:07:03	-11:20:16	4.5	EC	FSR 1190	Froebrich, Scholz & Raftery (2007)
225.48	-2.57	7:05:18	-12:19:44	4	EC	BDS 96	Bica et al. (2003b)
259.27	-2.61	8:22:22	-41:36:14	3	EC	Majaess 100	Majaess (2013)
259.29	-3.04	8:20:32	-41:51:47	3	EC	Majaess 98	Majaess (2013)
259.33	-2.55	8:22:49	-41:37:10	4	EC	Majaess 101	Majaess (2013)
259.50	-2.57	8:23:15	-41:46:06	6	EC	Majaess 104	Majaess (2013)
259.60	-2.98	8:21:45	-42:04:55	10	EC	Majaess 99	Majaess (2013)
259.61	-2.70	8:23:00	-41:55:45	9	EC	Majaess 103	Majaess (2013)
259.76	-2.84	8:22:52	-42:07:58	5	EC	DBS 18	Dutra et al. (2003)
260.76	0.66	8:41:07	-40:52:05	6	EC	MLG 1	Massi et al. (2000)
260.93	0.11	8:39:20	-41:19:53	3.5	EC	MLG 3	Massi et al. (2000)
263.53	-0.35	8:46:04	-43:39:43	6	EC	DBS 24	Dutra et al. (2003)
264.19	0.18	8:50:40	-43:50:44	8	EC	FSR 1424	Froebrich, Scholz & Raftery (2007)
264.23	-0.85	8:46:20	-44:31:16	5	EC	MLG 15	Massi et al. (2000)
264.32	-0.18	8:49:33	-44:10:47	1.0	EC	MLG 16	Massi et al. (2000)
264.47	-0.27	8:49:41	-44:21:31	4.5	EC	BH 54	van den Bergh & Hagen (1975)
264.67	-0.28	8:50:21	-44:30:43	1.7	EC	MLG 18	Massi et al. (2003)
264.73	0.26	8:52:55	-44:12:39	5	EC	FSR 1432	Froebrich, Scholz & Raftery (2007)
264.99	0.99	8:56:56	-43:56:30	7	EC	DBS 29	Dutra et al. (2003)
266.16	1.14	9:01:54	-44:43:32	6	EC	DBS 30	Dutra et al. (2003)
270.67	-2.45	9:03:43	-50:28:32	13	EC	Majaess 109	Majaess (2013)
276.96	-2.04	9:34:42	-54:40:26	6	EC	BH 75	van den Bergh & Hagen (1975)
281.76	-2.02	10:01:22	-57:43:10	4.5	EC	DBS 40	Dutra et al. (2003)
281.84	-1.61	10:03:40	-57:26:38	6	EC	Majaess 116	Majaess (2013)

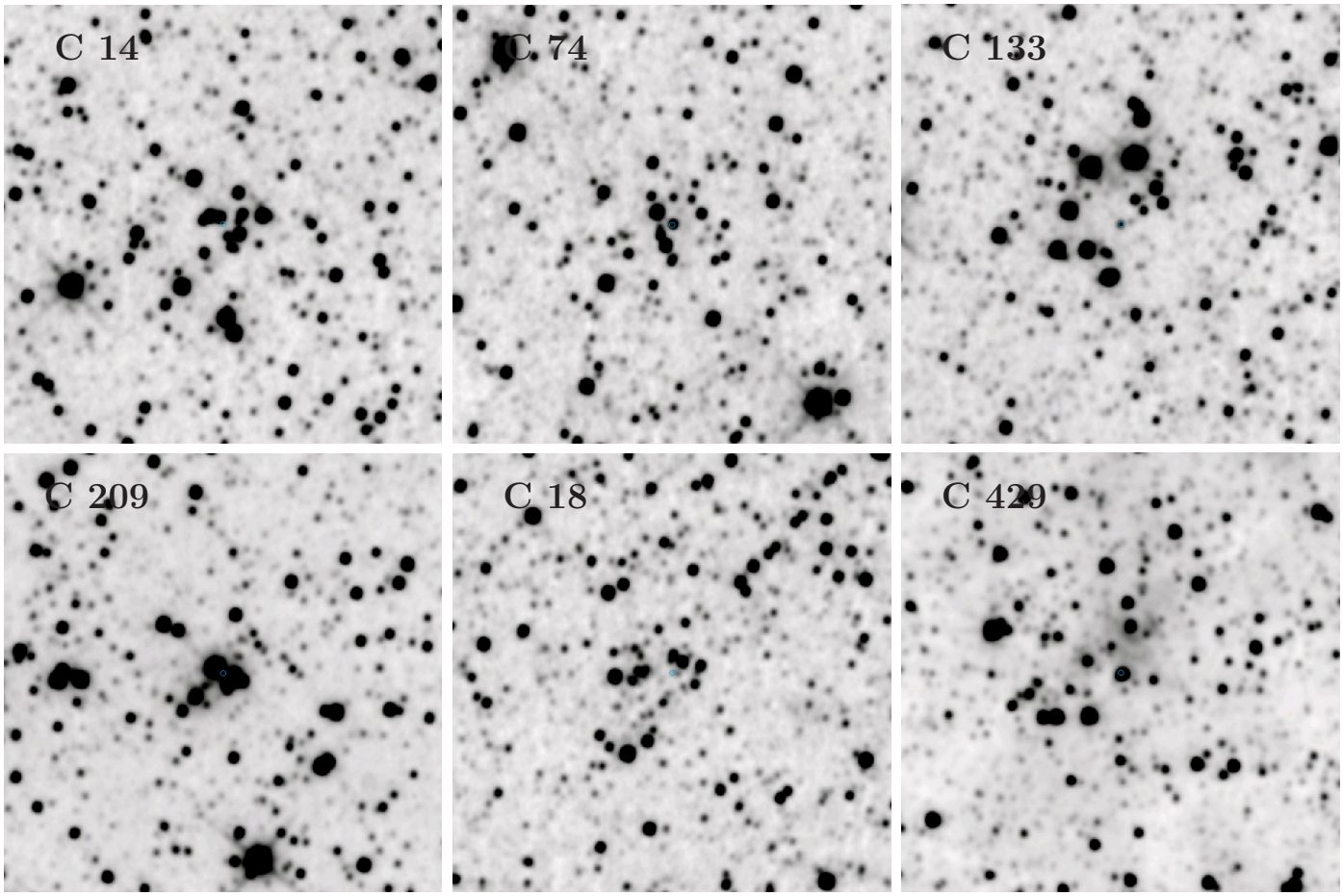

Figure 6 Examples of clusters in the test sub-sample. Top panels: W2 images ($10' \times 10'$) centred on C 14, C 74, and C 133. Bottom panels: the same for C 209, C 18, and C 429.

Table 3 Derived fundamental parameters for a test sample of 14 star clusters from Table 1.

Cluster	phase	α(2000)	δ(2000)	A_V	Age	$d_\odot$	R_{GC}	x_{GC}	y_{GC}	z_{GC}
---	---	($^\circ$ $'$ $''$)	(mag)	(Myr)	(kpc)	(kpc)	(kpc)	(kpc)	(kpc)	
(1)	(2)	(3)	(4)	(5)	(6)	(7)	(8)	(9)	(10)	(11)
C 14	EC	5:10:50	36:39:45	3.57 ± 0.2	3 ± 2	2.8 ± 0.26	9.95 ± 0.26	-9.93 ± 0.26	0.50 ± 0.05	-0.09 ± 0.01
C 18	EC	5:30:30	36:39:53	2.28 ± 0.2	2 ± 1	5.66 ± 0.54	12.85 ± 0.53	-12.82 ± 0.53	0.81 ± 0.08	-0.14 ± 0.01
C 64	EGr	6:08:49	13:09:38	4.27 ± 0.2	1 ± 1	3.8 ± 0.4	10.9 ± 0.5	-10.9 ± 0.5	-1.1 ± 0.1	-0.22 ± 0.02
C 74	EC	6:29:55	12:32:30	4.27 ± 0.2	3 ± 2	3.83 ± 0.27	10.9 ± 0.34	-10.83 ± 0.34	-1.27 ± 0.12	0.07 ± 0.01
C 133	EC	6:54:54	-3:21:39	2.28 ± 0.2	10 ± 5	3.26 ± 0.3	10.0 ± 0.25	-9.85 ± 0.25	-1.93 ± 0.18	-0.04 ± 0.01
C 149	EC	6:59:46	-3:36:33	1.49 ± 0.2	2 ± 1	9.1 ± 2.0	15.5 ± 1.8	-14.45 ± 1.8	-5.47 ± 0.57	0.03 ± 0.01
C 209	EC	6:59:12	-11:58:49	4.46 ± 0.2	2 ± 1	4.1 ± 0.5	10.53 ± 0.28	-10.13 ± 0.28	-2.86 ± 0.27	-0.27 ± 0.03
C 245	EC	8:25:16	-43:26:30	3.67 ± 0.2	1 ± 1	3.94 ± 0.40	8.6 ± 0.3	-7.8 ± 0.1	-3.9 ± 0.4	-0.22 ± 0.02
C 260	EC	8:30:24	-44:27:09	2.28 ± 0.2	2 ± 1	4.50 ± 0.43	9.0 ± 0.22	-7.8 ± 0.1	-4.45 ± 0.42	-0.24 ± 0.02
C 292	EC	9:14:28	-47:24:01	3.47 ± 0.2	1 ± 1	3.86 ± 0.37	8.21 ± 0.17	-7.25 ± 0.01	-3.86 ± 0.37	0.06 ± 0.01
C 353	EC	9:35:39	-54:11:40	3.47 ± 0.2	1 ± 1	4.23 ± 0.40	7.9 ± 0.2	-6.7 ± 0.1	-4.2 ± 0.4	-0.12 ± 0.01
C 394	EC	9:58:12	-56:08:24	1.98 ± 0.2	1 ± 1	5.12 ± 0.50	8.1 ± 0.3	-6.3 ± 0.1	-5.1 ± 0.5	-0.09 ± 0.01
C 399	EC	9:58:12	-56:27:03	5.46 ± 0.2	1 ± 1	3.0 ± 0.30	7.3 ± 0.2	-6.7 ± 0.1	-2.94 ± 0.3	-0.07 ± 0.01
C 429	EGr	10:04:07	-57:37:50	3.27 ± 0.2	1 ± 1	5.0 ± 0.50	7.9 ± 0.3	-6.2 ± 0.1	-4.9 ± 0.5	-0.15 ± 0.01

Table Notes. Col. 3: A_V in the cluster central region. Col. 4: age, from 2MASS photometry. Col. 5: distance from the Sun. Col. 6: R_{GC} calculated using $R_\odot = 7.2$ kpc for the distance of the Sun to the Galactic centre (Bica et al., 2006). Cols. 7 - 9: Galactocentric components.

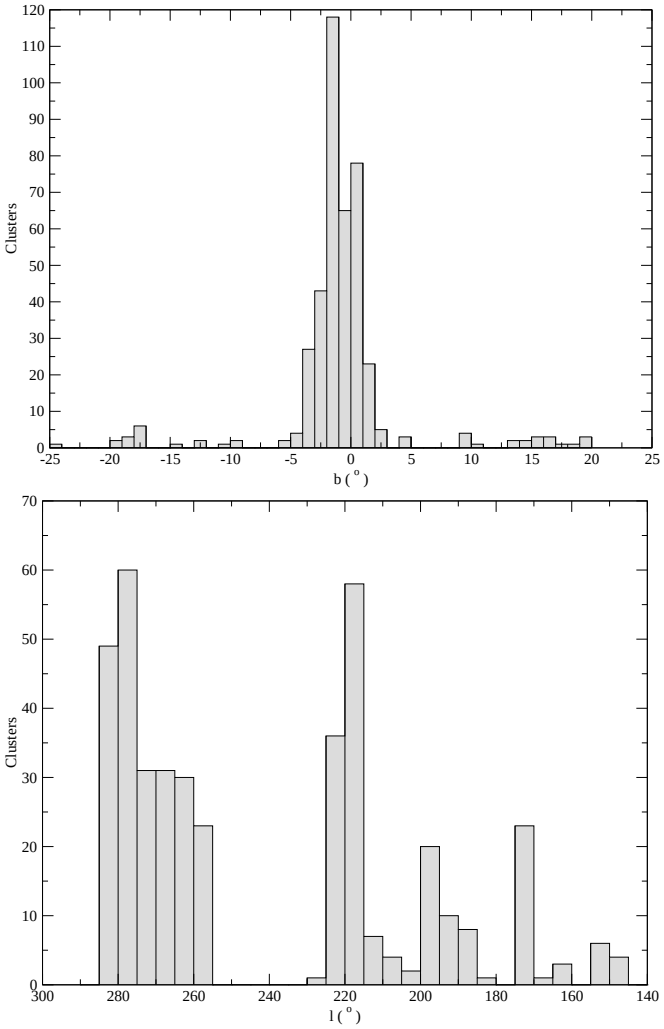

Figure 7 Distribution of the new clusters and candidates in Galactic latitude (top panel) and longitude (bottom panel).

3. Cluster structure and dust distribution

One of us (D. C.) carried out the cluster search and discovered 437 objects. The first 20 entries are listed in Table 1. The entire list is available in the online version of the paper. Table 1 shows the ranges of ℓ and b , so that most of the present survey was carried out in the 3rd Quadrant. Fig. 7 shows histograms of ℓ and b, while the Fig. 8 shows the $\ell \times b$ distribution of the new clusters and candidates. The present objects are mostly projected within small Galactic latitude values, as expected for a peaked thin disk recent stellar cluster formation. As a cautionary remark, the dips along longitude (Figs. 7 and 8) reflect more where we searched clusters than any intrinsic distribution. The sample does not intend to be complete in any sense. The distribution in Fig. 8 of populated areas and excursions that we made to search for the clusters suggest that a large number of ECs and other classes are yet to be found.

Star clusters show a variety of structures that depend on their evolutionary phase. They are formed as embedded clusters and their morphology in the earliest stage is tightly associated with the formation process, reflecting the morphology of the gas in their natal molecular clouds (Lada & Lada, 2003; Cartwright & Whitworth, 2004). Well known embedded cluster-forming regions are radially concentred or present a fractal-like structure with small ECs (Schmeja et al., 2008; Sánchez et al, 2010; Lomax et al., 2010; Camargo, Bonatto & Bica, 2011, 2012). These substructures are quickly erased by dynamical effects forming a massive cluster by coalescence or being completely dissolved in the field. On the other hand, some of them may evolve to individual clusters, forming a group of clusters or aggregate (Feigelson et al., 2011; Camargo, Bonatto & Bica, 2011, 2012). In the early ages substructured clusters and EC aggregates appear to be more able to survive the primordial gas expulsion than those centrally concentred (Kruijssen et al., 2012). ECs may present an expanding bubble generated by OB stars (Lee et al., 2012), some of which may develop subsequently a second generation of stars, and possibly a second generation of ECs, by means of sequential star formation.

The stellar systems analysed in this work present diversified morphologies. ECs have a core as a rule. The core may be stellar, dusty or dusty/stellar, suggesting that a collapse has occurred. EGrs have in general little central concentration. ECs and EGrs appear to be in general related to dust emission in bubbles or winds.

In Fig. 1 we show representative WISE images of ECs found in this study (C 62, C 72, C 258, C 44, C 284, and C 288). These clusters present evident stellar-density contrast with respect to the background. C 62 and C 44 are ECs with prominent dust/stellar cores.

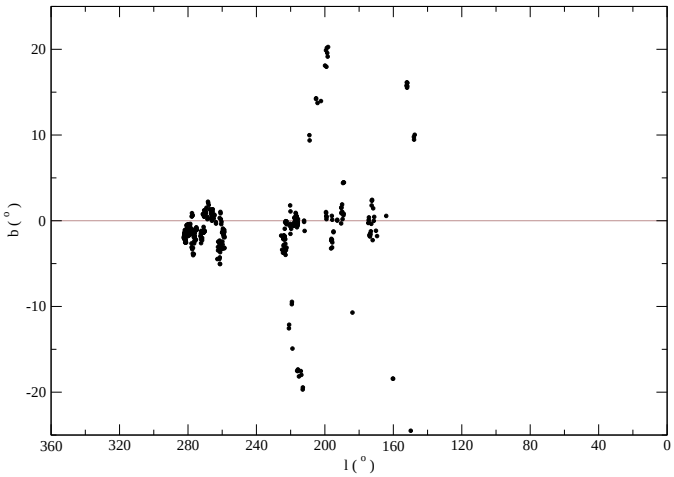

Figure 8 Galactic distribution of the new clusters and candidates.

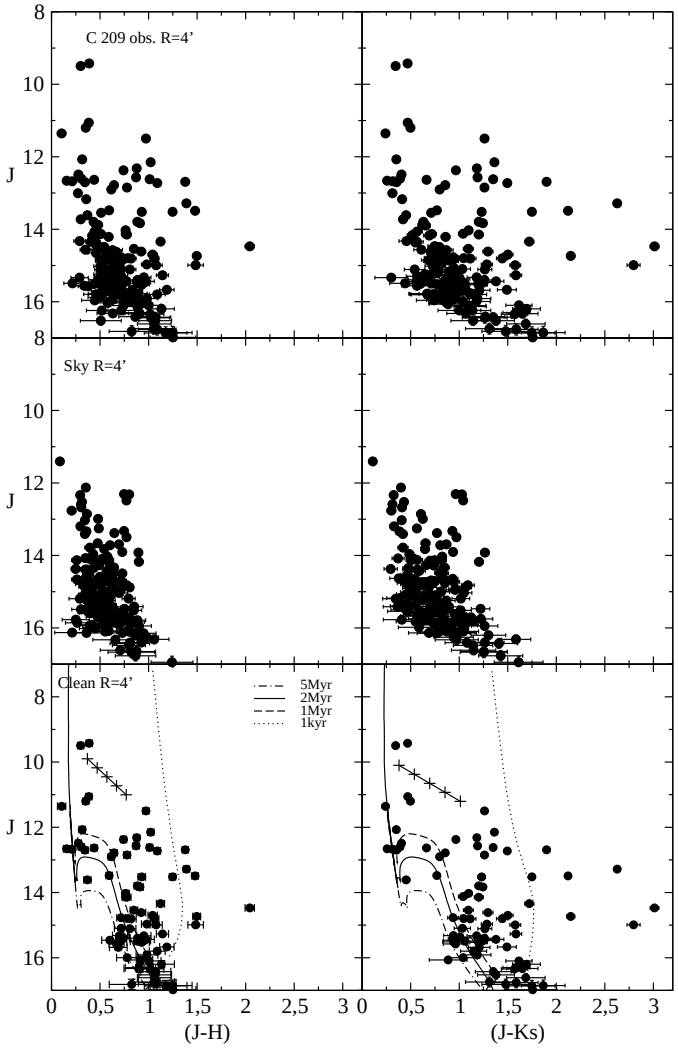

Figure 9 Band combinations in the colour-magnitude diagrams. 2MASS CMDs extracted from the central region of C 209. Top panels: observed CMDs $J \times (J-H)$ (left) and $J \times (J-K_s)$ (right). Middle panels: equal area comparison field. Bottom panels: field star decontaminated CMDs fitted with MS and PMS Padova isochrones. We also present the reddening vector for $A_V = 0$ to 5.

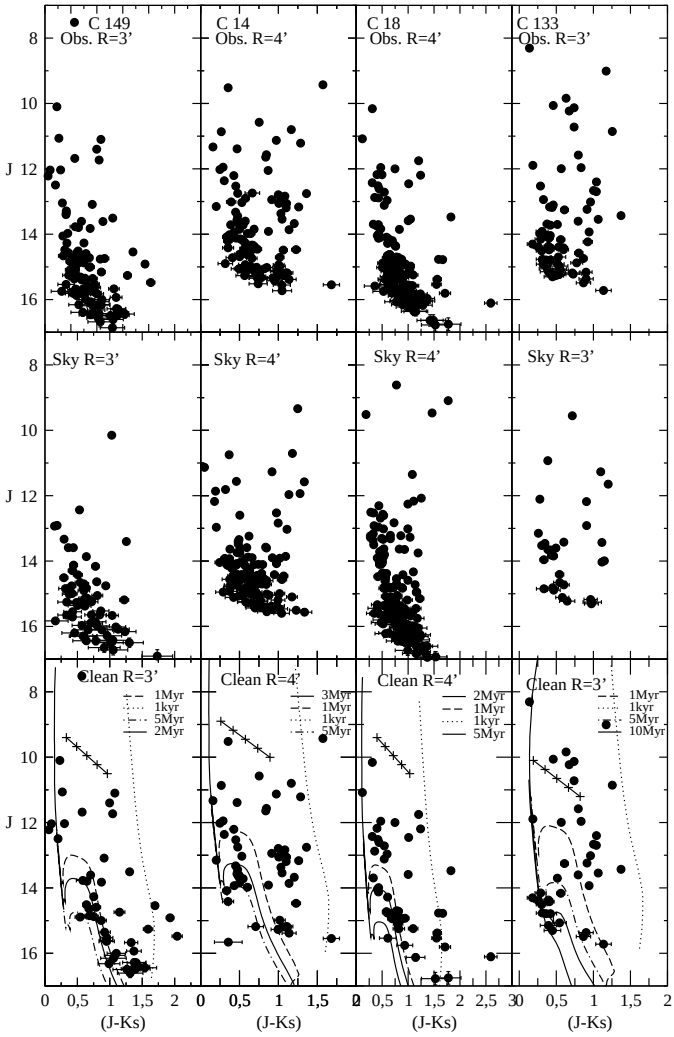

Figure 10 Colour-magnitude diagrams for the test subsample. 2MASS CMDs for the clusters C 149, C 14, C 18, and C 133. Top panels: observed CMDs $J \times (J-K_s)$. Middle panels: equal area comparison field. Bottom panels: field star decontaminated CMDs fitted with MS and PMS Padova isochrones. We show the reddening vector for $A_V = 0$ to 5.

Fig. 3 shows standard RGB images of representative objects in the sample (C 245, C 253, C 40, C 292, C 241, and C 39).

Fig. 4 shows interesting filamentary cluster-forming clouds. The s-shaped distribution of stars in C 260 may be linked to the remaining gas in the filamentary structure. The pair C 217 and C 213 are forming in a gas filament. C 217 presents an elongated stellar distribution aligned with the filament. It appears that the elongated shape of ECs in Fig. 4 is related to the primordial nebular structure.

In Fig. 5 we show some remarkable objects. C 201 presents a prominent structure resembling a diamond ring. C 178 is an EC-forming, which appears to be undergoing powerful wind shocks. C 219 together with C 218 and C 222 (in the same panel) form a probable group of clusters. They are aligned, probably as a consequence of the gas dynamics. The dust in C 219 shows a twisted filamentary structure.

The WISE RGB images of some presently discovered clusters, e.g., C 39, C 40, C 253, C 292, and C 260 (Figs. 3 and 4) show Extended Green Objects (EGOs), which are considered to be young stellar object (YSO) candidates (Churchwell et al., 2006, 2007; Zavagno et al., 2007; Cyganowski et al., 2012; Deharveng et al., 2010, and references therein). EGOs are often associated with infrared dark clouds (IRDCs) that are the precursors of cluster-forming clumps (Carey et al., 2000; Rathborne et al., 2010).

We conclude that dust enshrouded stellar clusters and

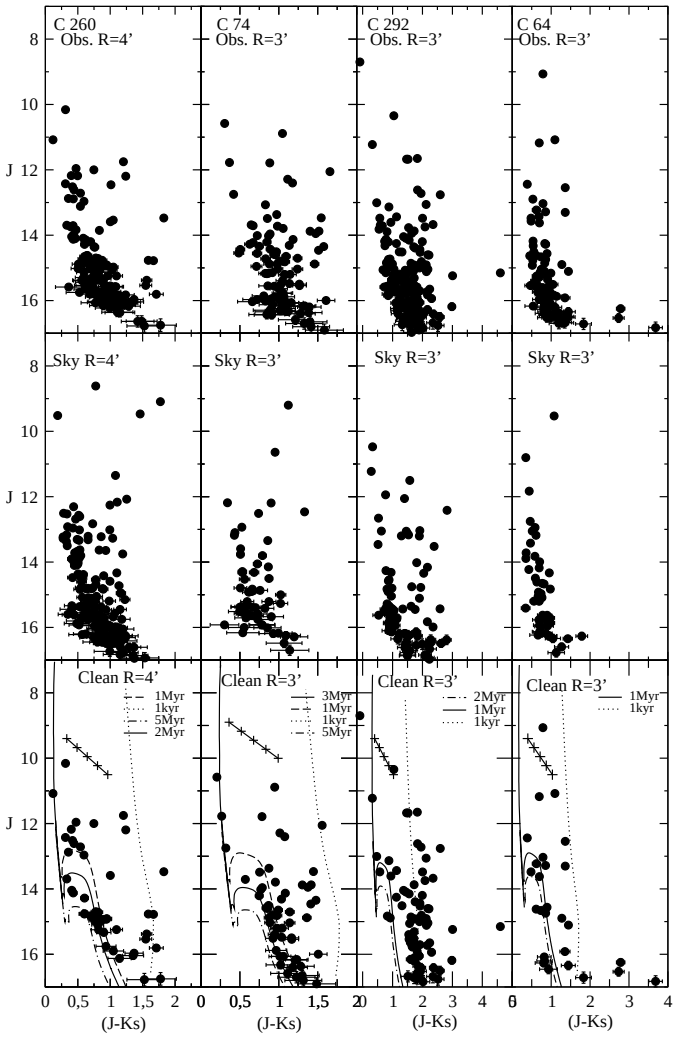

Figure 11 Same as Fig. 10 for the ECs C 260, C 74, C 292, and the EGr C 64.

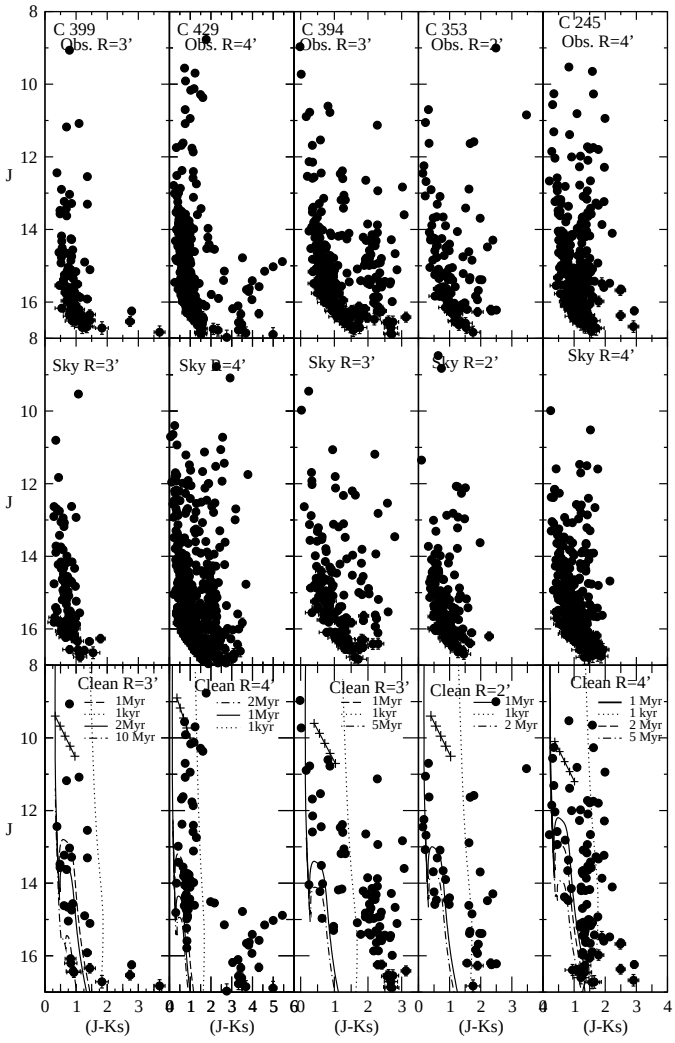

Figure 12 Same as Fig. 10 for the ECs C 245, C 353, C 394, C 399, and the EGr C 429.

aggregates in this work show a variety of projected stellar and dust distributions, and inferences can be made about star forming processes and stages.

4. 2MASS photometry and analytical tools

In this Section we present the tools to test whether a representative sub-sample of 14 WISE candidates (Table 2) are physical stellar clusters. We employ 2MASS[4] photometry (Skrutskie et al., 2006) in the J, H and K_s bands, extracted in circular concentric regions centred on the coordinates given in Table 3. 2MASS gives an adequate spatial and photometric uniformity required for wide extractions in view of a consistent field star decontamination. The analytical tools have been widely applied to stellar clusters in our previous papers, and below we refer to them for details on the methods.

[4]The Two Micron All Sky Survey, available at *www..ipac.caltech.edu/2mass/releases/allsky/*

Aiming to uncover the intrinsic CMD morphology from the foreground/background stars, we applied a field-star decontamination procedure (Bonatto & Bica, 2007a). The decontamination algorithm developed by one of us (C.B.) is fully described in Bonatto & Bica (2007b) and Bica, Bonatto & Camargo (2008). In short, the CMD is divided into a 3D grid of cells with axes along the J magnitude and the $(J-H)$ and $(J-K_s)$ colours, then the expected number-density of field stars in a given cell is computed based on the number of comparison field stars. Subsequently, the expected number of field stars is subtracted from each cell, generating the decontaminated CMD.

Fundamental parameters are derived using the field decontaminated CMD fitted with MS and PMS Padova isochrones (Bressan et al., 2012). The derived parameters are the observed distance modulus $(m-M)_J$ and reddening $E(J-H)$, which converts to $E(B-V)$ and A_V with the relations $A_J/A_V = 0.276$, $A_H/A_V = 0.176$, $A_{K_s}/A_V = 0.118$, $A_J = 2.76 \times E(J-H)$ and $E(J-H) = 0.33 \times E(B-V)$ (Dutra, Santiago & Bica, 2002). We as-

sume a constant total-to-selective absorption ratio $R_V = 3.1$ (Cardelli, Clayton & Mathis, 1989). Decontaminated CMDs are shown in Figs. 9 to 12. The fundamental parameters are estimated by applying shifts to the isochrone set from the zero distance modulus and reddening to the best fit.

As a rule, a star cluster structure is studied by means of the stellar radial density profile (RDP). Usually, star clusters have RDPs following a power law profile (King, 1962; Wilson, 1975; Elson et al., 1987). However, ECs are often heavily embedded in their embryonic molecular cloud, which may absorb the near background and part of the cluster member stars. As a result, some ECs may present RDPs with decreasing density towards the cluster centre or bumps and dips (Lada & Lada, 2003; Camargo, Bonatto & Bica, 2011, 2012; Camargo, Bica & Bonatto, 2013). Some RDP irregularities appear to be intrinsic to the embedded evolutionary stage and related to a fractal-like structure (Lada & Lada, 2003; Camargo, Bonatto & Bica, 2011, 2012; Camargo, Bica & Bonatto, 2013). We thus argue that overdensities in general are not enough to describe ECs in the earliest stages (Fig. 13).

5. CMD and RDP analyses of 14 test objects

Fig. 6 shows WISE images of a representative subsample of objects analysed in this section. In Figs. 9 to 11 are show their CMDs. The upper panels give CMDs extracted from a circular area centred on the coordinates of each object (Table 1). The middle panels correspond to the comparison fields of equal area, and the bottom panels give the decontaminated CMDs. The derived fundamental parameters (*age, reddening, distance*) are in Table 3.

Most of the present ECs and EGrs are in an initial evolutionary phase, and cannot be fitted by King's profile (Fig. 13). Normally, we apply a colour magnitude filter to the observed photometry to enhance the RDP contrast relative to the background (e.g. Bonatto & Bica, 2007a, 2009, 2010, 2011b; Camargo, Bonatto & Bica, 2009, 2010, and references therein), but the decontaminated CMDs of the present clusters show extremely reddened stars so that the filter is not effective by discarding such stars.

Fig. 9 shows for illustrative purposes the $(J-H)$ and $(J-K_s)$ CMDs for C 209. This EC presents high absorption ($A_V \approx 4.5$ mag). The decontaminated CMDs show extremely reddened stars mainly in the $(J-K_s)$ colour.

Probably, differential reddening contributed to the IR excess, but part of it can be intrinsic to their evolutionary stage, because the most reddened stars as a rule occupy the cluster core on the WISE images. Most of them are probably EGOs. In this sense, WISE is sensitive to the youngest stars in Class 0, which are still accreting material (Wright et al., 2010).

In Fig. 10 we show $(J-K_s)$ CMDs for C 149, C 14, C 18, and C 133, respectively. C 149 was initially classified as ECC, but based on the decontaminated CMD we now confirm it as EC. The best-fitting Padova MS and PMS isochrones suggest an age of 2 ± 1 Myr, a distance from the Sun of $d_\odot = 9.1$ kpc, and a distance from the Galactic centre of $R_{GC} = 15.45 \pm 1.8$ kpc. C 14 is recognised as a cluster by the presence of a core and combination of MS and PMS sequences in the decontaminated CMD. The estimated age is 3±2 Myr for $d_\odot = 2.8 \pm 0.26$ kpc. The RDP of C 14 (Fig. 13) presents a high density contrast to the field suggesting a cluster. The decontaminated CMD of the EC C 18 presents extremely reddened stars, again suggesting a cluster initial evolutionary stage. We derived an age of 2 ± 1 Myr and $d_\odot = 5.6 \pm 0.5$ kpc. The RDP of C 18 is also irregular with the background density centrally decreasing. The prominent C 133 has decontaminated CMD and RDP suggesting a cluster. We derive for C 133 an age of 10 ± 5 and $d_\odot = 3.3 \pm 0.3$ kpc. In the early age range ECs may be centrally concentrated with $R \sim 1$ pc (Parmentier & Pfalzner, 2012; Camargo, Bica & Bonatto, 2013).

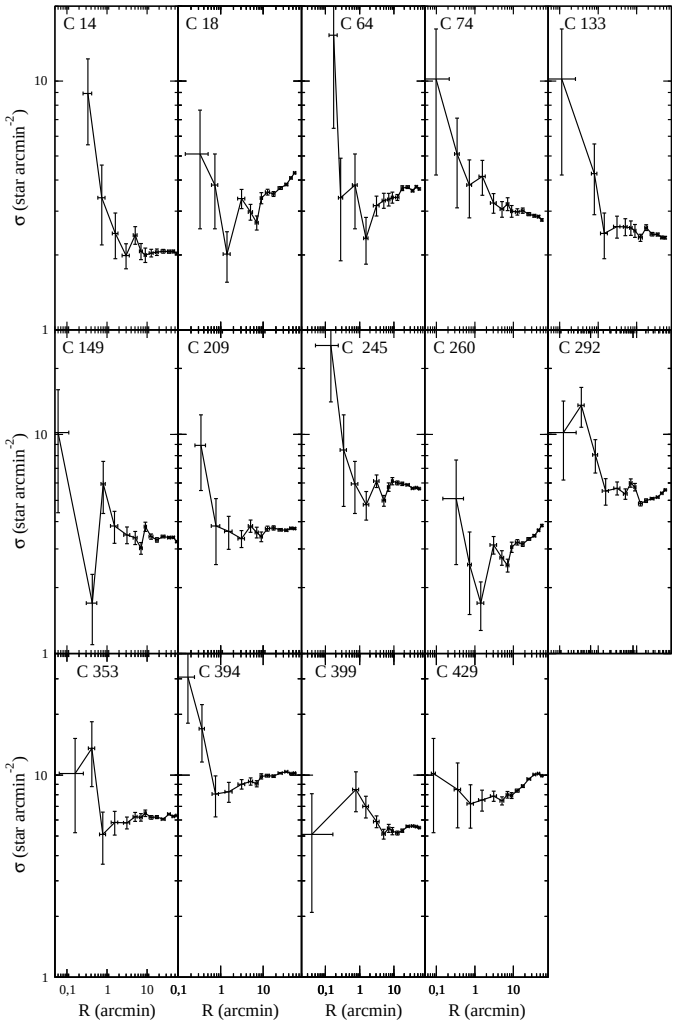

Figure 13 Radial density profiles for the embedded clusters and stellar groups in the test sub-sample.

Fig. 11 provides CMDs of C 260, C 74, C 292, and C 64. The WISE image of C 260 (Fig. 5) shows very reddened stars, but they are absent in the 2MASS photometry. Nonetheless, the decontaminated CMD shows features of an EC. The best fit age using MS and PMS isochrones is 2 ± 1 Myr, which implies in a $d_{\odot} = 4.5 \pm 0.4$ kpc and $R_{GC} = 9 \pm 0.2$ kpc. The decontaminated CMD of C 74 is typical of ECs with a poorly populated MS and a well-defined PMS. The cluster presents an important absorption of $A_V \sim 4.27$ mag, age of 3 ± 2 Myr, and $d_{\odot} = 3.83 \pm 0.27$ kpc. The RDP of C 74 is constrasted with respect to the background. C 292 is an EC with age of 1 ± 1 Myr and $d_{\odot} = 3.86 \pm 0.37$ kpc. The decontaminated CMD shows a prominent PMS with very reddened stars. Despite a dip in the inner RDP region, the structure of C 292 points to a cluster. The EGr C 64 also presents extremely reddened stars (Fig. 11). The decontaminated CMD points to an early age and the RDP is irregular, but shows a central peak.

Fig. 12 shows the CMDs for C 245, C 353, C 394, C 399, and the EGr C 429. The best fit of MS and PMS Padova isochrones provides an age of 1 ± 1 for these objects.

Some clusters appear to show an age spread, arising possibly from the merge of two generations of ECs or cluster-forming clumps (e.g. C 14 and C 133, Fig. 10).

We conclude from this chapter's analyses of CMDs and density profiles that this representative subsample is made up of star clusters, in general in their cold gas and dust embryonic cloud. This in turn reinforces expectations that the present list of 437 objects will become a major source for future studies of star cluster early evolutionary stages.

6. Concluding remarks

We report the discovery on WISE images of 437 Galactic star clusters, stellar groups, and candidates, mostly in the 3rd Galactic Quadrant. They are as a rule deeply embedded in their natal molecular clouds. Out of the 437 objects, 297 ($\sim 67.9\%$) were classified as embedded clusters, 23 ($\sim 5.3\%$) as candidates, 90 ($\sim 20.8\%$) as embedded stellar groups, and the remaining 27 ($\sim 6.2\%$) as open cluster candidates. We analysed in detail a subsample of 14 clusters by means of 2MASS photometry to probe their nature. We derived CMD fundamental cluster parameters for them. Radial density profiles do not follow a King's law, as expected for such young clusters. Most of them are very young (~ 1 Myr) , and in part present decontaminated CMDs with extremely reddened stars, comparable to those in infrared dark clouds that are the precursors of ECs.

The present catalogue of newly found embedded clusters and alike objects will certainly become a major object source for future studies of star cluster formation and early evolution.

Acknowledgements: We thank an anonymous referee for important comments and suggestions. This publication makes use of data products from the Two Micron All Sky Survey and Wide-field Infrared Survey Explorer. The first is a joint project of the University of Massachusetts and the Infrared Processing and Analysis Centre/California Institute of Technology. The second, is a joint project of the University of California, Los Angeles, and the Jet Propulsion Laboratory/California Institute of Technology. Both funded by the National Aeronautics and Space Administration and the National Science Foundation. We acknowledge support from INCT-A and CNPq (Brazil).

References

Acker, A., Ochsenbein, F., Stenholm, B., et al. 1992, ESO-Strasbourg Catalogue of Galactic Planetary Nebulae, Munich (ESO)
Adams, F. C, Myers, P. 2001, ApJ, 553, 744
Avedisova, V. S. 2002, ARep, 46, 193
Bica, E., Dutra, C. M., & Barbuy, B. 2003a, A&A, 397, 177
Bica, E., Dutra, C.M, Soares, J., Barbuy, B. 2003b, A&A, 404, 223
Bica, E., Bonatto, C. 2005, A&A, 443, 465
Bica, E., Bonatto, C., Barbuy, B. & Ortolani, S. 2006, A&A, 450, 105
Bica, E., Bonatto, C. & Camargo, D. 2008, MNRAS, 385, 349
Bobylev, V. V., Bajkova, A. T., & Lebedeva, S. V., 2007, As. Lett., 33, 720
Bobylev, V. V. & Bajkova, A. T., 2014, MNRAS, 437, 1549
Bonatto C., Kerber L. O., Bica E., Santiago B. X., 2006, A&A, 446, 121
Bonatto C. & Bica E. 2007a, A&A, 473, 445
Bonatto C. & Bica E. 2007b, MNRAS, 477, 1301
Bonatto C. & Bica E. 2009, MNRAS, 397, 1915
Bonatto, C. & Bica, E. 2010, A&A, 516, 81
Bonatto C. & Bica E. 2011, A&A, 530, 32
Borissova, J., Bonatto, C., Kurtev, R., Clarke, J. R. A., Peñaloza, F., Sale, S. E., Minniti, D., Alonso-García, J. et al. 2011, A&A, 532, 131
Bressan, A., Marigo, P., Girardi, L., Salasnich, B., Dal Cero, C., Rubele, S., & Nanni, A. 2012, MNRAS, 427, 127b
Bukowiecki, L., Maciejewski, G., Konorski, P., Strobel, A. 2011, A&A, 61, 231
Camargo, D., Bonatto, C. & Bica, E. 2009, A&A, 508, 211
Camargo, D., Bonatto, C. & Bica, E. 2010, A&A, 521, 42
Camargo, D., Bonatto, C. & Bica, E. 2011, MNRAS, 416, 1522
Camargo, D., Bonatto, C. & Bica, E. 2012, MNRAS, 423, 1940
Camargo, D., Bica, E. & Bonatto, C. 2013, MNRAS, 432, 3349
Cardelli, J. A., Clayton, G.C. & Mathis, J. S. 1989, ApJ., 345, 245
Carey, S. J., Feldman, P. A., Redman, R. O., Egan, M. P., MacLeod, J. M., & Price, S. D. 2000, ApJ, 543, 157
Cartwright A., Whitworth A. P., 2004, MNRAS, 348, 589
Churchwell, E., Povich, M. S., Allen, D., Taylor, M. G., Meade, M. R., Babler, B. L., Indebetouw, R., Watson, C. et al. 2006, ApJ, 649, 759
Churchwell, E., Watson, D. F., Povich, M. S., Taylor, M. G., Babler, B. L., Meade, M. R., Benjamin, R. A., Indebetouw, R., & Whitney, B. A. 2007, ApJ, 670, 428
Cyganowski, C. J., Whitney, B. A., Holden, E., Braden, E., Brogan, C. L., Churchwell, E., Indebetouw, R., Watson, D. F., et al., 2008, AJ, 136, 2391
Deharveng, L., Schuller, F., Anderson, L. D., Zavagno, A., Wyrowski, F., Menten, K. M., Bronfman, L., Testi, L. et al. 2010, A&A, 523, 6D
de Wit, W. J., Testi, L., Palla, F., Vanzi, L., Zinnecker, H. 2004, A&A, 425, 937
Dias, W. S., Alessi, B. S., Moitinho, A., & Lépine, J. R. D. 2002, A&A, 389, 871
Dutra, C.M., Santiago, B.X. & Bica, E. 2002, A&A, 383, 219
Dutra, C.M., Bica, E., Soares, J., Barbuy, B. 2003, A&A, 400, 533

Elson, R.A.W., Fall, S.M. & Freeman, K.C. 1987, ApJ, 323, 54
Feigelson E. D., Getman, K. V., Townsley, L. K., Broos, P. S., Povich, M. S., Garmire, G. P., King, R. R., Montmerle, T., et al., 2011, ApJS, 194, 9
Friel, E.D. 1995, ARA&A, 33, 381
Froebrich, D., Scholz, A., & Raftery, C. L.2007, MNRAS, 374, 399
Glushkova, E. V., Koposov, S. E., Zolotukhin, I. Y., Beletsky, Y. V., Vlasov, A. D. & Leonova, S. I., 2010, Ast. Letters, 36, 75
Hodapp, K.-W. 1994, ApJS, 94, 615
Ivanov, V. D., Borissova, J., Pessev, P., Ivanov, G. R. & Kurtev, R. 2002, A&A, 394, 1
Kharchenko, N.V., Piskunov, A.E. Röser, S., Schilbach, E. & Scholz, R.-D. 2005a, A&A, 438, 1163
Kharchenko, N.V., Piskunov, A.E. Röser, S., Schilbach, E. & Scholz, R.-D. 2005b, A&A, 440, 403
King, I. 1962, AJ, 67, 471
Koposov, S. E., Glushkova, E. V. & Zolotukhin, I.Yu. 2007, A&A, 486, 771
Krone-Martins, A., Soubiran, C., Ducourant, C., Teixeira, R., Le Campion, J. F., 2010, A&A, 516, 3
Kruijssen, J. M. D., Maschberger, T., Moeckel, N., Clarke, C. J., Bastian, N., & Bonnell, I. A. 2012, MNRAS, 419, 841K
Kronberger, M., Teutsch, P., Alessi, B., Steine, M., Ferrero, L., Graczewski, K., Juchert, M., Patchick, D., et al., 2006, A&A, 447, 921
Kumar, M. S. N., Keto, E. & Clerkin, E. 2006, A&A, 449, 1033
Lada, E. A., Depoy, D. L., Evans, II, N. J. & Gatley, I. 1991, ApJ, 371, 171
Lada, C.J. & Lada, E.A. 2003, ARA&A, 41, 57
Lee, E. J., Murray, N. & Rahman, M. 2012, ApJ, 752, 146
Lomax, O., Whitworth, A. P. & Cartwright, A.T. 2011, MNRAS, 412, 627
Maciejewski, G., Niedzielski, A. 2007, A&A, 467, 1065
Majaess, D. 2013 Ap&SS, 344, 175
Massi, F., Lorenzetti, D., Giannini, T., Vitali, F., 2000, A&A, 353, 598
Massi, F., Lorenzetti, D., Giannini, T., 2003, A&A, 399, 147
Mercer, E. P. 2005, ApJ, 635, 560
Mermelliod, J. C. 1996, in The Origins, Evolution, and Destinies of Binary Stars in Clusters, ed. E. F. Milone, & J. C. Mermilliod, ASP Conf. Ser., 90, 475
Parmentier, G. & Pfalzner, S. 2012, arXiv:1211.1383v1
Piskunov A. E., Kharchenko N. V., Röser S., Schilbach E., Scholz R.-D., 2006, A&A, 445, 545
Puga, E., Hony, S., Neiner, C., Lenorzer, A., Hubert, A.-M., Waters, L. M., Cusano, F., Ripepi, V. 2009, A&A, 503, 107
Rathborne, J. M., Jackson, J. M., & Simon, R. 2010, ApJ, 641, 389
Sánchez, N., Anez, N., Alfaro, E. J. & Odekon, M. C. 2010, arXiv:1007.3621v1
Schmeja, S., Kumar, M. S. N. & Ferreira, B. 2008, MNRAS, 389, 1209
Sharma, S., Pandey, A. K., Ogura, K., Mito, H., Tarusawa, K., Sagar, R. 2006, AJ,132, 1669
Skrutskie, M.F. et al. 2006, AJ, 131, 1163
Soares, J. B., Bica, E. , 2002, A&A, 388, 172
van den Bergh, S., Hagen, G. L., 1975, AJ, 80, 11
Wilson, C.P. 1975, AJ, 80, 175
Wright, E. L., Eisenhardt, P. R. M., Mainzer, A. K. et al. 2010, AJ, 140, 1868
Zavagno, A., Pomarès, M., Deharveng, L., Hosokawa, T., Russeil, D., & Caplan, J. 2007, A&A, 472, 835
Ybarra, J. E., Lada, E. A., Román-Zúñiga, C. G., Balog, Z., Wang, J., & Feigelson, E. D. 2013, ApJ, 769, 140

Appendix A. Online material

We carried out a search that provided 437 new star clusters, stellar groups, and candidates. The first 20 entries are listed in Table 1 and Table A.4 provide the full list of newly found star clusters.

Table A.4. The list of discovered star clusters or candidates.

Target	ℓ	b	α(2000)	δ(2000)	Size	Type	Avend.	Comments
	(°)	(°)	(h m s)	(° ′ ″)	(′)			
(1)	(2)	(3)	(4)	(5)	(6)	(7)	(8)	(9)
Camargo 1	147.52	10.03	4 : 44 : 32	61 : 12 : 03	8 × 8	EC	n	loose core, prominent
Camargo 2	147.88	9.46	4 : 42 : 50	60 : 33 : 46	9 × 9	EC	n	loose core, impressive
Camargo 3	147.99	9.79	4 : 45 : 28	60 : 41 : 25	10 × 10	EC	n	loose core
Camargo 4	149.83	-24.50	2 : 47 : 55	32 : 13 : 07	8 × 8	OCC	n	
Camargo 5	151.83	15.69	5 : 42 : 49	60 : 51 : 31	7 × 7	EC	n	prominent
Camargo 6	151.84	16.06	5 : 45 : 34	61 : 01 : 36	8 × 8	EC	n	loose core
Camargo 7	151.96	16.11	5 : 46 : 19	60 : 56 : 45	12 × 12	ECC	n	
Camargo 8	151.97	15.52	5 : 42 : 05	60 : 39 : 31	5 × 5	EC	n	core, impressive
Camargo 9	152.12	16.14	5 : 47 : 08	60 : 49 : 12	6 × 6	EGr	n	
Camargo 10	152.30	15.76	5 : 45 : 02	60 : 29 : 36	6 × 6	EGr	n	
Camargo 11	160.11	-18.43	3 : 41 : 22	31 : 54 : 37	4 × 4	EC	n	core
Camargo 12	160.28	-18.42	3 : 41 : 58	31 : 48 : 45	6 × 6	EC	n	core, prominent
Camargo 13	164.15	0.56	5 : 03 : 50	42 : 22 : 15	5 × 5	EC	n	impresssive dusty
Camargo 14	169.52	-1.79	5 : 10 : 50	36 : 39 : 45	6 × 6	EC	n	core
Camargo 15	170.13	-1.17	5 : 15 : 04	36 : 31 : 54	7 × 7	EGr	n	
Camargo 16	171.17	0.45	5 : 24 : 41	36 : 36 : 16	5 × 5	EC	y	impressive
Camargo 17	171.43	-0.01	5 : 23 : 30	36 : 07 : 49	7 × 7	EC	n	core
Camargo 18	171.77	1.45	5 : 30 : 30	36 : 39 : 53	7 × 7	EC	n	impressive
Camargo 19	172.08	-2.26	5 : 16 : 18	34 : 18 : 54	4 × 4	EGr	y	wind, cirrus, impressive
Camargo 20	172.42	2.44	5 : 36 : 23	36 : 39 : 41	5 × 5	EC	n	impressive
Camargo 21	172.53	2.35	5 : 36 : 17	36 : 31 : 07	7 × 7	EC	y	prominent
Camargo 22	172.69	1.78	5 : 34 : 21	36 : 04 : 14	4 × 4	EC	n	prominent, core
Camargo 23	172.86	-0.36	5 : 26 : 03	34 : 45 : 11	6 × 6	EC	n	core, impressive winds
Camargo 24	173.14	-1.24	5 : 23 : 15	34 : 01 : 35	2 × 2	EGr	y	shocks
Camargo 25	173.51	-1.58	5 : 22 : 55	33 : 31 : 52	6 × 6	EC	y	impressive, shocks
Camargo 26	172.53	2.35	5 : 36 : 17	36 : 31 : 07	6 × 6	EC	y	wind
Camargo 27	173.56	-1.52	5 : 23 : 19	33 : 31 : 42	2 × 2	EC	y	shocks, in Do 18b
Camargo 28	173.58	-1.57	5 : 23 : 09	33 : 28 : 42	2 × 2	EC	y	
Camargo 29	173.59	-1.62	5 : 22 : 58	33 : 26 : 40	2 × 2	EGr	y	
Camargo 30	173.61	-1.72	5 : 22 : 39	33 : 22 : 18	5 × 5	EC	y	core
Camargo 31	173.68	-1.84	5 : 22 : 21	33 : 14 : 39	3 × 3	EGr	n	winds
Camargo 32	173.85	-1.67	5 : 23 : 28	33 : 11 : 52	3 × 3	EC	y	winds
Camargo 33	173.86	-1.73	5 : 23 : 18	33 : 09 : 19	10 × 10	EGr	y	winds
Camargo 34	174.26	-0.23	5 : 30 : 18	33 : 39 : 47	4 × 4	ECC	n	faint core, distant?
Camargo 35	174.28	0.39	5 : 32 : 53	33 : 59 : 05	6 × 6	EC	n	core
Camargo 36	174.41	0.08	5 : 31 : 57	33 : 42 : 02	6 × 6	EC	n	core, impressive
Camargo 37	174.66	-0.26	5 : 31 : 14	33 : 18 : 48	6 × 6	EC	n	impressive, diffuse core
Camargo 38	183.87	-10.71	5 : 15 : 18	19 : 52 : 42	7 × 7	OCC	n	
Camargo 39	188.86	4.46	6 : 22 : 20	23 : 24 : 47	5 × 5	EC	n	impressive, wind
Camargo 40	189.43	4.40	6 : 23 : 15	22 : 52 : 45	6 × 6	EC	y	impressive, dusty core
Camargo 41	189.00	0.82	6 : 08 : 46	21 : 33 : 52	3 × 3	EGr	y	
Camargo 42	189.14	0.64	6 : 08 : 23	21 : 21 : 27	7 × 7	EC	n	winds, impressive
Camargo 43	189.15	4.48	6 : 22 : 59	23 : 10 : 08	4 × 4	EGr	y	dusty core, 2nd generation?
Camargo 44	189.68	0.18	6 : 07 : 47	20 : 39 : 32	5 × 5	EC	y	impressive, core
Camargo 45	189.87	1.04	6 : 11 : 23	20 : 54 : 19	8 × 8	EC	n	impressive, core
Camargo 46	189.93	1.90	6 : 14 : 46	21 : 16 : 01	10 × 10	OCC	n	core
Camargo 47	190.13	0.98	6 : 11 : 46	20 : 39 : 22	7 × 7	EC	n	winds, impressive
Camargo 48	190.24	0.92	6 : 11 : 41	20 : 31 : 43	7 × 7	EC	n	impressive, wind
Camargo 49	190.29	0.87	6 : 11 : 38	20 : 27 : 23	7 × 7	EC	n	loose
Camargo 50	190.32	1.56	6 : 14 : 15	20 : 45 : 20	8 × 8	EC	n	core
Camargo 51	190.44	1.50	6 : 14 : 17	20 : 37 : 33	10 × 10	EGr	n	
Camargo 52	190.50	-0.31	6 : 07 : 40	19 : 42 : 03	7 × 7	EC	n	bubble, impressive, core
Camargo 53	192.76	0.01	6 : 13 : 25	17 : 52 : 40	4 × 4	EGr	y	core
Camargo 54	192.79	0.11	6 : 13 : 52	17 : 53 : 48	5 × 5	EC	y	prominent
Camargo 55	194.97	-1.25	6 : 13 : 13	15 : 20 : 13	3.5 × 2.5	EC	y	impressive
Camargo 56	194.97	-1.34	6 : 12 : 56	15 : 17 : 25	6 × 6	EC	n	shock prominent
Camargo 57	195.65	-2.53	6 : 09 : 57	14 : 07 : 24	6 × 6	EC	n	asymmetric?
Camargo 58	195.68	0.11	6 : 19 : 36	15 : 21 : 21	7 × 7	EC	y	core, impressive
Camargo 59	195.77	-3.12	6 : 08 : 04	13 : 43 : 55	7 × 7	OCC	n	core
Camargo 60	195.86	-2.22	6 : 11 : 29	14 : 05 : 09	4 × 4	EGr	n	few stars, prominent
Camargo 61	195.94	0.57	6 : 21 : 48	15 : 20 : 37	5 × 5	EGr	n	
Camargo 62	196.19	-2.11	6 : 12 : 31	13 : 51 : 17	5 × 5	EC	y	impressive, core
Camargo 63	196.30	-2.31	6 : 12 : 01	13 : 39 : 36	8 × 8	EC	n	
Camargo 64	196.36	-3.23	6 : 08 : 49	13 : 09 : 38	6 × 6	EGr	y	winds
Camargo 65	198.11	20.27	7 : 40 : 56	21 : 48 : 37	5 × 5	OCC	n	
Camargo 66	198.36	19.15	7 : 36 : 51	21 : 09 : 56	6 × 6	OCC	n	small core
Camargo 67	198.64	19.57	7 : 38 : 57	21 : 05 : 17	8 × 8	OCC	n	
Camargo 68	198.86	20.16	7 : 41 : 38	21 : 06 : 52	3 × 3	ECC	n	
Camargo 69	198.96	0.46	6 : 27 : 13	12 : 37 : 22	5 × 5	EC	n	core

Table A.4 (continued)

Target	ℓ	b	α(2000)	δ(2000)	Size	Type	Avend.	Comments
	(°)	(°)	(h m s)	(° ′ ″)	(′)			
(1)	(2)	(3)	(4)	(5)	(6)	(7)	(8)	(9)
Camargo 70	199.09	17.96	7 : 33 : 19	20 : 04 : 03	8 × 8	OCC	n	small core
Camargo 71	199.10	0.19	6 : 26 : 30	12 : 22 : 04	7 × 7	EC	n	impressive
Camargo 72	199.22	0.53	6 : 27 : 58	12 : 25 : 38	6 × 6	EC	n	impressive
Camargo 73	199.27	0.90	6 : 29 : 25	12 : 33 : 03	7 × 7	EGr	n	
Camargo 74	199.34	1.01	6 : 29 : 55	12 : 32 : 30	6 × 6	EC	n	impressive
Camargo 75	199.35	19.88	7 : 41 : 15	20 : 34 : 57	5 × 5	SFN	n	dusty core? star forming?
Camargo 76	199.90	18.10	7 : 35 : 09	19 : 24 : 44	10 × 10	OCC	n	
Camargo 77	202.29	13.96	7 : 23 : 12	15 : 38 : 04	8 × 8	EGr	n	
Camargo 78	204.30	13.74	7 : 25 : 47	13 : 46 : 09	6 × 6	OCC	n	loose core
Camargo 79	208.92	9.37	7 : 17 : 44	7 : 47 : 50	7 × 7	OC	n	loose core, impressive
Camargo 80	209.05	9.98	7 : 20 : 10	7 : 57 : 19	4 × 4	ECC	n	
Camargo 81	211.58	-1.13	6 : 44 : 56	0 : 41 : 16	7 × 7	EGr	n	wind
Camargo 82	211.66	-1.05	6 : 45 : 23	0 : 38 : 55	8 × 8	EGr	y	wind
Camargo 83	211.78	-1.50	6 : 43 : 59	0 : 20 : 37	6 × 4	EC	n	
Camargo 84	211.79	-1.35	6 : 44 : 32	0 : 23 : 49	6 × 6	EC	n	
Camargo 85	211.82	-1.44	6 : 44 : 17	0 : 19 : 51	6 × 6	EC	n	
Camargo 86	211.85	-1.19	6 : 45 : 14	0 : 25 : 00	8 × 8	EC	y	wind, prominent
Camargo 87	211.89	-1.28	6 : 44 : 59	0 : 20 : 47	6 × 6	EGr	y	
Camargo 88	211.90	-1.20	6 : 45 : 16	0 : 22 : 20	4 × 4	EC	y	
Camargo 89	211.92	-0.98	6 : 46 : 07	0 : 27 : 17	8 × 8	EGr	n	wind
Camargo 90	211.92	-1.53	6 : 44 : 09	0 : 12 : 11	6 × 6	EC	n	winds, prominent
Camargo 91	211.95	-1.42	6 : 44 : 36	0 : 13 : 47	7 × 7	EC	y	impressive morphology
Camargo 92	211.99	-1.13	6 : 45 : 40	0 : 19 : 51	7 × 7	EC	y	
Camargo 93	212.03	-0.40	6 : 48 : 22	0 : 37 : 19	7 × 7	EC	y	prominent dusty core
Camargo 94	212.04	-1.08	6 : 45 : 58	0 : 18 : 15	6 × 6	EGr	y	winds
Camargo 95	212.10	-1.28	6 : 45 : 23	0 : 09 : 19	7 × 7	EGr	n	scattered
Camargo 96	212.11	-0.97	6 : 46 : 28	0 : 17 : 30	7 × 7	EC	n	
Camargo 97	212.11	-1.11	6 : 46 : 00	0 : 13 : 42	7 × 7	EGr	y	wind
Camargo 98	212.14	-0.14	6 : 49 : 30	0 : 38 : 46	6 × 6	EC	n	prominent, wind, core
Camargo 99	212.14	0.01	6 : 50 : 02	0 : 42 : 34	6 × 6	EC	n	prominent
Camargo 100	212.15	-1.42	6 : 44 : 57	0 : 03 : 05	8 × 8	EGr	y	impressive, winds
Camargo 101	212.18	-1.34	6 : 45 : 18	0 : 03 : 30	6 × 6	EC	n	prominent, winds
Camargo 102	212.22	-1.02	6 : 46 : 31	0 : 10 : 05	5 × 5	EC	y	bubble
Camargo 103	212.26	-1.27	6 : 45 : 42	0 : 01 : 08	7 × 7	EC	n	small loose core
Camargo 104	212.28	-0.62	6 : 48 : 03	0 : 17 : 56	5 × 5	EC	y	impressive
Camargo 105	212.35	-0.92	6 : 47 : 07	0 : 06 : 07	6 × 6	EC	y	winds
Camargo 106	212.42	-1.13	6 : 46 : 30	−0 : 03 : 35	6 × 6	EC	y	bubble
Camargo 107	212.45	-0.98	6 : 47 : 04	−0 : 01 : 08	7 × 7	EC	y	long core
Camargo 108	212.86	-19.45	5 : 41 : 30	−8 : 40 : 14	8 × 8	EC	n	impressive
Camargo 109	212.95	-19.69	5 : 40 : 49	−8 : 51 : 21	7 × 7	OCC	n	
Camargo 110	212.53	-0.74	6 : 48 : 05	0 : 00 : 58	6 × 6	EC	n	prominent
Camargo 111	212.64	-0.79	6 : 48 : 07	−0 : 06 : 12	6 × 6	EC	n	
Camargo 112	213.75	-17.98	5 : 48 : 21	−8 : 47 : 32	7 × 7	OCC	n	
Camargo 113	214.05	-17.54	5 : 50 : 28	−8 : 51 : 36	5 × 5	OCC	n	
Camargo 114	215.16	-18.16	5 : 50 : 05	−10 : 04 : 34	7 × 7	EGr	n	
Camargo 115	215.73	0.20	6 : 57 : 15	−2 : 24 : 12	7 × 7	EC	n	
Camargo 116	215.75	-17.35	5 : 54 : 01	−10 : 14 : 29	4.5 × 4.5	EC	n	
Camargo 117	215.79	-0.27	6 : 55 : 42	−2 : 40 : 02	7 × 7	EGr	n	
Camargo 118	215.86	-17.54	5 : 53 : 30	−10 : 24 : 38	3 × 2	EGr	n	2nd generation, wind
Camargo 119	215.87	-17.49	5 : 53 : 42	−10 : 23 : 52	8 × 8	OCC	n	
Camargo 120	215.91	-0.56	6 : 54 : 52	−2 : 54 : 27	10 × 10	ECC	n	
Camargo 121	216.00	-0.13	6 : 56 : 35	−2 : 47 : 11	4 × 4	ECC	n	
Camargo 122	216.02	-0.38	6 : 55 : 42	−2 : 55 : 20	7 × 7	OCC	n	
Camargo 123	216.06	-0.12	6 : 56 : 44	−2 : 50 : 19	6 × 6	EC	n	core
Camargo 124	216.11	-0.25	6 : 56 : 22	−2 : 56 : 24	5 × 5	EGr	n	PN A 18 3.5 NW
Camargo 125	216.14	-0.24	6 : 56 : 25	−2 : 57 : 44	9 × 9	EC	n	
Camargo 126	216.15	-0.47	6 : 55 : 38	−3 : 04 : 46	10 × 10	OCC	n	
Camargo 127	216.18	0.04	6 : 57 : 30	−2 : 52 : 12	10 × 10	ECC	y	
Camargo 128	216.18	0.12	6 : 57 : 48	−0 : 50 : 26	5 × 5	EGr	n	
Camargo 129	216.22	-17.51	5 : 54 : 13	−10 : 42 : 37	6 × 6	OCC	n	
Camargo 130	216.23	-0.50	6 : 55 : 40	−3 : 09 : 46	8 × 8	EC	n	prominent dusty core
Camargo 131	216.23	-0.11	6 : 57 : 03	−2 : 59 : 06	8 × 8	EC	n	
Camargo 132	216.26	-0.24	6 : 56 : 38	−3 : 04 : 10	7 × 7	ECC	n	prominent
Camargo 133	216.32	-0.76	6 : 54 : 54	−3 : 21 : 39	10 × 10	EC	n	prominent
Camargo 134	216.36	-0.28	6 : 56 : 43	−3 : 10 : 45	7 × 7	EC	n	wind
Camargo 135	216.41	0.10	6 : 58 : 08	−3 : 02 : 50	8 × 8	ECC	n	
Camargo 136	216.41	0.18	6 : 58 : 26	−3 : 00 : 52	9 × 9	ECC	n	
Camargo 137	216.45	0.52	6 : 59 : 43	−2 : 53 : 20	9 × 9	EC	n	
Camargo 138	216.51	-0.06	6 : 57 : 45	−3 : 12 : 28	10 × 10	ECC	n	wind

Table A.4 (continued)

Target	ℓ	b	α(2000)	δ(2000)	Size	Type	Avend.	Comments
	(°)	(°)	(h m s)	(° ′ ″)	(′)			
(1)	(2)	(3)	(4)	(5)	(6)	(7)	(8)	(9)
Camargo 139	216.64	0.26	6 : 59 : 08	−3 : 10 : 50	2.5 × 2.5	EC	n	
Camargo 140	216.66	-0.46	6 : 56 : 36	−3 : 31 : 55	8 × 8	ECC	n	
Camargo 141	216.68	0.54	7 : 00 : 12	−3 : 05 : 33	7 × 7	EC	n	
Camargo 142	216.89	0.28	6 : 59 : 40	−3 : 23 : 42	3 × 2.5	EC	n	
Camargo 143	216.92	0.03	6 : 58 : 49	−3 : 31 : 55	2 × 1.5	SFN	n	dust ring with bright spots
Camargo 144	216.92	-0.34	6 : 57 : 30	−3 : 42 : 03	10 × 10	EC	n	prominent
Camargo 145	216.92	0.82	7 : 01 : 40	−3 : 10 : 37	2 × 2	EC	n	
Camargo 146	217.03	-0.14	6 : 58 : 26	−3 : 42 : 19	4 × 4	ECC	y	
Camargo 147	217.05	0.91	7 : 02 : 12	−3 : 14 : 57	5 × 5	EC	y	
Camargo 148	217.09	0.34	7 : 00 : 15	−3 : 32 : 40	8 × 8	EC	n	prominent
Camargo 149	217.09	0.20	6 : 59 : 46	−3 : 36 : 33	3 × 2	EC	n	shock, few stars
Camargo 150	217.11	0.43	7 : 00 : 36	−3 : 31 : 06	2 × 2	EC	n	prominent
Camargo 151	217.11	-0.19	6 : 58 : 24	−3 : 48 : 18	10 × 10	EC	y	
Camargo 152	217.15	-0.03	6 : 59 : 03	−3 : 46 : 04	5 × 3.5	EC	n	
Camargo 153	217.19	-0.07	6 : 58 : 58	−3 : 49 : 07	2 × 2	EC	y	core of a larger cluster?
Camargo 154	217.21	0.48	7 : 00 : 58	−3 : 35 : 14	5 × 5	EC	n	
Camargo 155	217.27	-0.34	6 : 58 : 08	−4 : 00 : 45	10 × 10	EC	n	
Camargo 156	217.32	0.32	7 : 00 : 35	−3 : 45 : 23	5 × 5	EC	n	
Camargo 157	217.40	0.09	6 : 59 : 56	−3 : 56 : 03	6 × 6	EGr	n	
Camargo 158	217.42	0.32	7 : 00 : 46	−3 : 51 : 15	1.5 × 1.5	EC	y	
Camargo 159	217.42	0.28	7 : 00 : 38	−3 : 51 : 41	2 × 2	EC	y	shock induced?
Camargo 160	217.45	0.35	7 : 00 : 57	−3 : 51 : 34	2.5 × 2.5	EC	y	shock induced? impressive
Camargo 161	217.62	-0.15	6 : 59 : 29	−4 : 14 : 25	2 × 1	EC	y	bubble, subcluster or 2nd generation of BDS 89
Camargo 162	217.67	1.14	7 : 04 : 10	−3 : 41 : 26	5 × 5	EC	n	small cl. and large dust cores
Camargo 163	217.90	0.35	7 : 01 : 46	−4 : 15 : 25	2.5 × 2.5	EC	n	
Camargo 164	217.96	-0.51	6 : 58 : 49	−4 : 42 : 12	5 × 5	EC	n	
Camargo 165	218.10	-0.36	6 : 59 : 35	−4 : 46 : 01	4 × 4	EC	y	
Camargo 166	218.15	-0.57	6 : 58 : 57	−4 : 53 : 56	5 × 5	EC	y	include 1 SE possible subcluster, rel. [G84d]1-3
Camargo 167	218.16	-0.58	6 : 58 : 55	−4 : 54 : 53	1 × 1	EC	y	subcluster or in pair
Camargo 168	218.16	-0.29	6 : 59 : 58	−4 : 46 : 54	6 × 6	EC	y	
Camargo 169	218.74	-0.47	7 : 00 : 24	−5 : 22 : 42	5.5 × 5.5	EGr	n	
Camargo 170	218.93	-14.91	6 : 08 : 19	−11 : 57 : 17	8 × 8	OCC	n	core
Camargo 171	219.24	-9.46	6 : 28 : 53	−9 : 52 : 08	5 × 5	EC	n	prominent
Camargo 172	219.32	-9.74	6 : 28 : 00	−10 : 03 : 43	10 × 10	EC	y	prominent
Camargo 173	219.68	-0.94	7 : 00 : 26	−6 : 26 : 02	4.5 × 4.5	OCC	n	
Camargo 174	220.10	1.09	7 : 08 : 27	−5 : 52 : 40	6 × 6	ECC	n	
Camargo 175	220.14	-1.53	6 : 59 : 10	−7 : 06 : 31	7 × 7	OCC	n	
Camargo 176	220.25	-0.36	7 : 03 : 33	−6 : 40 : 30	4.5 × 4.5	EGr	n	
Camargo 177	220.30	1.79	7 : 11 : 19	−5 : 43 : 49	5 × 5	EC	n	core
Camargo 178	220.46	-0.61	7 : 03 : 02	−6 : 58 : 26	8 × 8	EC	y	inc shock
Camargo 179	220.89	-12.13	6 : 21 : 56	−12 : 29 : 22	6 × 6	EC	n	prominent
Camargo 180	221.00	-12.55	6 : 20 : 34	−12 : 46 : 16	5 × 5	OCC	n	core
Camargo 181	221.29	0.07	7 : 07 : 02	−7 : 24 : 10	3 × 2	SFN	n	small dust neb, bright in W3, star forming?
Camargo 182	222.28	-0.41	7 : 07 : 08	−8 :: 30 : 16	8 × 8	OCC	n	
Camargo 183	222.43	-3.14	6 : 57 : 35	−9 : 52 : 41	3 × 3	EGr	n	
Camargo 184	222.43	-0.12	7 : 08 : 28	−8 : 30 : 00	4 × 4	EC	n	shock origin, 1st generation
Camargo 185	222.47	-0.06	7 : 08 : 44	−8 : 30 : 20	3 × 2	EC	n	shock induced,2nd generation
Camargo 186	222.74	-0.32	7 : 08 : 19	−8 : 51 : 58	8 × 8	OCC	n	core
Camargo 187	222.74	-3.42	6 : 57 : 09	−10 : 16 : 55	4 × 4	EC	n	
Camargo 188	222.95	-0.05	7 : 09 : 40	−8 : 55 : 59	5 × 5	OCC	n	core
Camargo 189	222.98	-3.98	6 : 55 : 32	−10 : 44 : 59	1.5 × 1.5	EC	n	
Camargo 190	223.12	-2.69	7 : 00 : 30	−10 : 17 : 37	4.5 × 4.5	ECC	n	bubble?
Camargo 191	223.13	-2.15	7 : 02 : 28	−10 : 03 : 09	5 × 5	EC	n	prominent
Camargo 192	223.16	-3.51	6 : 57 : 34	−10 : 42 : 00	7 × 7	ECC	n	
Camargo 193	223.20	-3.16	6 : 58 : 56	−10 : 34 : 46	5 × 5	OCC	n	prominent core
Camargo 194	223.24	-0.18	7 : 09 : 46	−9 : 14 : 50	5 × 5	EC	n	prominent
Camargo 195	223.45	-0.94	7 : 07 : 25	−9 : 46 : 57	5 × 5	EC	n	shock, impressive, winds
Camargo 196	223.51	-1.78	7 : 04 : 31	−10 : 13 : 25	5 × 5	EC	n	
Camargo 197	223.51	-3.75	6 : 57 : 22	−11 : 07 : 04	1.5 × 1.5	EGr	n	
Camargo 198	223.54	-1.86	7 : 04 : 15	−10 : 16 : 57	4.5 × 4.5	EC	n	
Camargo 199	223.62	-1.89	7 : 04 : 18	−10 : 22 : 32	6 × 6	EGr	n	winds
Camargo 200	223.71	-1.90	7 : 04 : 25	−10 : 27 : 17	4 × 4	EC	n	
Camargo 201	223.71	-2.20	7 : 03 : 20	−10 : 35 : 20	2 × 2	EC	y	diamond ring, shock impressive
Camargo 202	223.85	-1.87	7 : 04 : 48	−10 : 33 : 43	8 × 8	ECC	n	
Camargo 203	224.01	-1.70	7 : 05 : 43	−10 : 37 : 58	5 × 4	EC	n	prominent
Camargo 204	224.09	-2.94	7 : 01 : 22	−11 : 16 : 02	4.5 × 4.5	EC	n	bubble
Camargo 205	224.09	-2.84	7 : 01 : 44	−11 : 13 : 20	4 × 4	EGr	n	shock
Camargo 206	224.14	-1.94	7 : 05 : 05	−10 : 51 : 39	5 × 5	EC	n	
Camargo 207	224.34	-2.14	7 : 04 : 44	−11 : 07 : 14	3 × 3	EC	n	shock

Table A.4 (continued)

Target	ℓ	b	α(2000)	δ(2000)	Size	Type	Avend.	Comments
	(°)	(°)	(h m s)	(° ′ ″)	(′)			
(1)	(2)	(3)	(4)	(5)	(6)	(7)	(8)	(9)
Camargo 208	224.35	-2.02	7 : 05 : 12	−11 : 04 : 36	6 × 6	EC	n	impressive
Camargo 209	224.48	-3.74	6 : 59 : 12	−11 : 58 : 49	10 × 10	EC	n	prominent core
Camargo 210	224.97	-3.39	7 : 01 : 22	−12 : 15 : 24	4.5 × 4.5	EC	n	prominent core
Camargo 211	225.55	-1.74	7 : 08 : 27	−12 : 01 : 06	10 × 10	EGr	n	
Camargo 212	258.61	-1.93	8 : 23 : 20	−40 : 39 : 58	5 × 5	EC	n	impressive, dusty core
Camargo 213	258.67	-3.16	8 : 18 : 07	−41 : 25 : 02	5 × 5	EC	n	prominent
Camargo 214	258.74	-1.31	8 : 26 : 23	−40 : 25 : 21	5 × 5	EGr	n	bubble, wind
Camargo 215	258.79	-1.09	8 : 27 : 32	−40 : 20 : 04	6 × 6	EC	n	core
Camargo 216	258.81	-1.80	8 : 24 : 30	−40 : 45 : 23	5 × 5	EGr	n	bubble
Camargo 217	258.82	-3.22	8 : 18 : 20	−41 : 34 : 45	4 × 3	EC	n	shock, wind, impressive
Camargo 218	259.05	-1.55	8 : 26 : 19	−40 : 48 : 39	5 × 5	EC	n	impressive, ring core
Camargo 219	259.08	-1.62	8 : 26 : 06	−40 : 52 : 35	5 × 5	EC	n	spiral wind,impressive
Camargo 220	259.08	-1.90	8 : 24 : 53	−41 : 02 : 21	5 × 5	EC	n	
Camargo 221	259.09	-1.78	8 : 25 : 27	−40 : 58 : 54	6 × 6	ECC	n	wind, impressive
Camargo 222	259.12	-1.74	8 : 25 : 44	−40 : 58 : 32	5 × 5	EC	n	prominent, wind
Camargo 223	259.14	-1.08	8 : 28 : 38	−40 : 36 : 33	5 × 5	EC	n	core
Camargo 224	259.24	-1.63	8 : 26 : 33	−41 : 00 : 36	3 × 3	EC	n	dusty core
Camargo 225	259.31	-1.62	8 : 26 : 49	−41 : 04 : 11	5 × 5	EGr	n	
Camargo 226	259.56	-0.92	8 : 30 : 36	−40 : 51 : 38	6 × 6	EC	n	prominent
Camargo 227	259.57	-1.03	8 : 30 : 11	−40 : 55 : 50	5 × 5	EC	n	
Camargo 228	259.57	-1.44	8 : 28 : 25	−41 : 10 : 08	5 × 5	EGr	y	
Camargo 229	259.64	-1.31	8 : 29 : 09	−41 : 08 : 58	7 × 7	EC	y	in Majaess 107, impressive, chain
Camargo 230	259.71	-1.27	8 : 29 : 32	−41 : 11 : 06	5 × 5	EC	y	in Majaess 107, bubble, shock
Camargo 231	259.73	-1.32	8 : 29 : 25	−41 : 14 : 01	5 × 5	EC	y	in Majess 107, winds
Camargo 232	259.77	-2.78	8 : 23 : 10	−42 : 06 : 07	5 × 5	EGr	n	bubble
Camargo 233	259.81	-3.26	8 : 21 : 09	−42 : 24 : 35	2.5 × 2.5	EC	n	impressive
Camargo 234	259.89	-2.43	8 : 25 : 05	−42 : 00 : 09	6 × 6	EGr	n	impressive, shock
Camargo 235	259.90	-1.39	8 : 29 : 38	−41 : 24 : 56	2 × 2	OCC	n	far OC?, also in 2MASS
Camargo 236	259.91	-1.33	8 : 29 : 56	−41 : 22 : 44	6 × 6	EGr	n	
Camargo 237	260.08	-1.38	8 : 30 : 14	−41 : 32 : 45	8 × 8	EGr	n	
Camargo 238	260.42	-0.12	8 : 36 : 44	−41 : 04 : 26	8 × 8	EC	n	shock
Camargo 239	260.54	-0.40	8 : 35 : 54	−41 : 20 : 21	6 × 6	EC	n	
Camargo 240	260.81	0.19	8 : 39 : 17	−41 : 11 : 30	7 × 7	EC	n	prominent
Camargo 241	260.91	-3.10	8 : 25 : 18	−43 : 13 : 19	8 × 8	EC	n	core
Camargo 242	260.95	0.87	8 : 42 : 36	−40 : 53 : 23	5 × 5	EGr	n	core
Camargo 243	260.96	-3.33	8 : 24 : 25	−43 : 23 : 45	9 × 9	EC	n	ring of stars
Camargo 244	261.04	1.03	8 : 43 : 34	−40 : 51 : 33	6 × 6	EC	n	prominent
Camargo 245	261.09	-3.23	8 : 25 : 16	−43 : 26 : 30	6 × 5	EC	n	prominent
Camargo 246	261.20	-3.67	8 : 23 : 39	−43 : 47 : 09	5 × 5	EGr	n	core
Camargo 247	261.26	-5.05	8 : 17 : 26	−44 : 36 : 48	7 × 7	EC	n	impressive wind
Camargo 248	261.32	-3.06	8 : 26 : 45	−43 : 32 : 07	6 × 6	EC	y	core
Camargo 249	261.33	-5.04	8 : 17 : 45	−44 : 40 : 02	7 × 7	EC	n	
Camargo 250	261.42	-4.28	8 : 21 : 31	−44 : 18 : 53	6 × 6	EC	n	core
Camargo 251	261.47	0.32	8 : 41 : 59	−41 : 38 : 18	8 × 8	EC	n	impressive
Camargo 252	261.54	-2.32	8 : 30 : 48	−43 : 17 : 02	8 × 7	EC	n	sequential star formation? bubble, winds, impressive
Camargo 253	261.56	-2.51	8 : 29 : 59	−43 : 24 : 45	5 × 5	EC	n	prominent
Camargo 254	261.58	-2.68	8 : 29 : 18	−43 : 31 : 18	6 × 6	EC	n	prominent
Camargo 255	261.59	-2.47	8 : 30 : 17	−43 : 24 : 38	3 × 3	EC	n	
Camargo 256	261.65	-4.47	8 : 21 : 25	−44 : 36 : 45	10 × 10	ECC	n	
Camargo 257	261.78	-3.04	8 : 28 : 20	−43 : 53 : 40	6 × 6	EC	n	winds
Camargo 258	262.36	-2.45	8 : 32 : 53	−44 : 01 : 29	6 × 6	EC	n	impressive
Camargo 259	262.41	-3.46	8 : 28 : 29	−44 : 38 : 54	6 × 4	ECC	n	
Camargo 260	262.45	-3.06	8 : 30 : 24	−44 : 27 : 09	8 × 8	EC	y	impressive,chain in W4
Camargo 261	262.84	-4.47	8 : 25 : 14	−45 : 35 : 10	6 × 6	EC	n	prominent
Camargo 262	263.61	-0.33	8 : 46 : 27	−43 : 42 : 48	8 × 8	EC	n	prominent
Camargo 263	263.71	-0.16	8 : 47 : 30	−43 : 41 : 18	7 × 7	EC	n	2 other nearby centers possible
Camargo 264	264.54	0.61	8 : 53 : 44	−43 : 50 : 33	7 × 7	EC	y	prominent
Camargo 265	264.54	0.70	8 : 54 : 07	−43 : 47 : 11	6 × 6	EC	n	
Camargo 266	264.97	0.26	8 : 53 : 46	−44 : 23 : 47	6 × 6	EC	n	impressive nuclear dust
Camargo 267	265.51	1.34	9 : 00 : 18	−44 : 06 : 08	8 × 8	EC	n	core, impressive
Camargo 268	265.68	1.07	8 : 59 : 47	−44 : 24 : 24	8 × 8	EC	n	prominent
Camargo 269	265.82	0.92	8 : 59 : 39	−44 : 36 : 39	7 × 7	EC	n	
Camargo 270	265.84	1.10	9 : 00 : 31	−44 : 30 : 48	6 × 6	EC	y	prominent, core
Camargo 271	265.92	0.24	8 : 57 : 10	−45 : 08 : 03	6 × 6	EGr	n	wind
Camargo 272	265.99	1.04	9 : 00 : 50	−44 : 40 : 00	6 × 6	EC	n	
Camargo 273	265.99	0.50	8 : 58 : 29	−45 : 01 : 02	13 × 13	EC	n	prominent
Camargo 274	266.02	0.00	8 : 56 : 28	−45 : 21 : 34	10 × 10	EC	n	wind, bubble, prominent, core, dust
Camargo 275	266.09	0.39	8 : 58 : 26	−45 : 10 : 07	6 × 6	EC	n	bubble
Camargo 276	266.18	0.33	8 : 58 : 29	−45 : 16 : 32	6 × 6	EC	n	bubble

Table A.4 (continued)

Target	ℓ	b	α(2000)	δ(2000)	Size	Type	Avend.	Comments
	(°)	(°)	(h m s)	(° ′ ″)	(′)			
(1)	(2)	(3)	(4)	(5)	(6)	(7)	(8)	(9)
Camargo 277	266.20	0.76	9 : 00 : 25	−45 : 00 : 04	6 × 6	EC	n	core
Camargo 278	266.23	0.88	9 : 01 : 00	−44 : 56 : 55	7 × 7	EC	y	core
Camargo 279	266.27	1.00	9 : 01 : 41	−44 : 53 : 52	6 × 6	EGr	n	
Camargo 280	266.27	1.10	9 : 02 : 09	−44 : 49 : 59	5 × 5	EGr	n	impressive mid IR core
Camargo 281	266.36	0.75	9 : 00 : 57	−45 : 08 : 03	7 × 7	EC	n	core
Camargo 282	266.42	1.32	9 : 03 : 36	−44 : 47 : 43	8 × 8	EC	n	
Camargo 283	266.51	0.22	8 : 59 : 15	−45 : 35 : 33	6 × 5	EC	n	impressive
Camargo 284	266.60	0.90	9 : 02 : 29	−45 : 12 : 35	7 × 7	EC	n	core,impressive
Camargo 285	267.45	1.33	9 : 07 : 34	−45 : 33 : 00	6 × 6	EC	n	impressive, core
Camargo 286	267.88	1.83	9 : 11 : 21	−45 : 31 : 48	5 × 5	EC	n	
Camargo 287	268.17	2.07	9 : 13 : 26	−45 : 34 : 29	8 × 8	EC	y	small core
Camargo 288	268.32	2.22	9 : 14 : 39	−45 : 35 : 01	5 × 5	EC	n	wind, impressive
Camargo 289	268.62	0.45	9 : 08 : 22	−47 : 01 : 04	8 × 8	EGr	n	
Camargo 290	268.65	0.18	9 : 07 : 19	−47 : 12 : 52	7 × 7	EC	n	impressive
Camargo 291	269.21	1.51	9 : 15 : 14	−46 : 42 : 57	6 × 6	EGr	n	central concentration
Camargo 292	269.61	0.94	9 : 14 : 28	−47 : 24 : 01	5 × 5	EC	n	impressive, winds
Camargo 293	269.67	1.07	9 : 15 : 18	−47 : 21 : 23	6 × 6	EGr	n	impressive, cirrus
Camargo 294	269.79	0.85	9 : 14 : 51	−47 : 35 : 21	6 × 6	EC	n	impressive
Camargo 295	269.87	0.78	9 : 14 : 50	−47 : 41 : 40	2 × 2	EGr	n	
Camargo 296	269.88	1.14	9 : 16 : 26	−47 : 27 : 20	6 × 6	EC	n	impressive
Camargo 297	269.97	0.84	9 : 15 : 34	−47 : 43 : 39	6 × 6	EC	n	impressive
Camargo 298	270.04	0.76	9 : 15 : 28	−47 : 49 : 47	6 × 6	EGr	n	winds
Camargo 299	270.20	1.05	9 : 17 : 22	−47 : 45 : 09	6 × 6	EC	n	winds
Camargo 300	270.25	-1.26	9 : 07 : 28	−49 : 22 : 01	8 × 8	EC	n	impressive
Camargo 301	270.33	0.81	9 : 16 : 52	−48 : 00 : 37	6 × 6	EGr	y	winds
Camargo 302	270.37	0.76	9 : 16 : 52	−48 : 04 : 15	3 × 3	EGr	n	wind
Camargo 303	270.37	-1.24	9 : 08 : 01	−49 : 26 : 57	7 × 7	EC	n	impressive
Camargo 304	270.39	-1.13	9 : 08 : 35	−49 : 23 : 12	6 × 6	EC	n	prominent
Camargo 305	270.45	-1.21	9 : 08 : 30	−49 : 29 : 18	5 × 5	EC	n	impressive, shock
Camargo 306	270.51	0.74	9 : 17 : 20	−48 : 11 : 08	5 × 5	EC	y	resolved dusty core, impressive
Camargo 307	270.53	1.22	9 : 19 : 29	−47 : 51 : 59	6 × 6	EC	n	bubble, impressive
Camargo 308	270.55	0.46	9 : 16 : 20	−48 : 24 : 41	10 × 8	EC	y	
Camargo 309	270.56	0.82	9 : 17 : 55	−48 : 10 : 03	6 × 6	EC	y	impressive
Camargo 310	270.68	-1.21	9 : 09 : 27	−49 : 38 : 50	6 × 6	EC	n	impressive, strong wind
Camargo 311	280.77	-1.06	9 : 59 : 49	−56 : 21 : 56	6 × 6	EC	n	dusty core
Camargo 312	270.77	0.61	9 : 17 : 54	−48 : 27 : 34	5 × 4	EC	y	
Camargo 313	270.82	-1.11	9 : 10 : 30	−49 : 41 : 27	7 × 7	EC	y	impressive, wind
Camargo 314	270.82	-1.40	9 : 09 : 10	−49 : 53 : 03	4 × 4	EC	n	
Camargo 315	270.88	-0.72	9 : 12 : 30	−49 : 28 : 00	5 × 5	EC	y	impressive, dusty core
Camargo 316	270.93	0.70	9 : 18 : 57	−48 : 30 : 56	7 × 7	EC	n	core
Camargo 317	270.95	-1.38	9 : 09 : 51	−49 : 58 : 05	6 × 6	EGr	n	bubble
Camargo 318	270.96	-1.11	9 : 11 : 06	−49 : 47 : 34	8 × 8	EC	n	prominent
Camargo 319	271.12	0.79	9 : 20 : 09	−48 : 35 : 00	8 × 8	ECC	n	
Camargo 320	271.33	0.77	9 : 20 : 58	−48 : 44 : 39	8 × 8	EC	n	impressive
Camargo 321	271.72	-2.00	9 : 10 : 17	−50 : 57 : 01	7 × 7	EC	n	prominent, wind
Camargo 322	271.73	-2.27	9 : 09 : 03	−51 : 08 : 45	4 × 4	EC	n	dusty core
Camargo 323	272.25	-1.19	9 : 16 : 17	−50 : 46 : 29	5 × 5	EC	n	impressive, wind, 2nd generation
Camargo 324	272.35	-2.61	9 : 10 : 08	−51 : 50 : 00	6 × 6	EC	n	binuclear, impressive, sequential
Camargo 325	272.40	-2.16	9 : 12 : 29	−51 : 33 : 10	7 × 7	EC	n	dusty core, impressive
Camargo 326	272.49	-1.49	9 : 15 : 59	−51 : 09 : 23	7 × 7	EC	n	bubble
Camargo 327	272.58	-1.73	9 : 15 : 16	−51 : 23 : 15	6 × 6	EC	n	impressive, dusty core
Camargo 328	272.70	-1.82	9 : 15 : 29	−51 : 32 : 27	6 × 6	EC	n	prominent
Camargo 329	274.92	-1.06	9 : 29 : 06	−52 : 33 : 40	7 × 7	EC	y	dusty core
Camargo 330	275.08	-0.85	9 : 30 : 48	−52 : 31 : 16	3 × 3	EC	n	subcluster
Camargo 331	275.09	-0.88	9 : 30 : 45	−52 : 33 : 10	12 × 12	EC	n	incl. subcluster
Camargo 332	275.07	-1.09	9 : 29 : 43	−52 : 41 : 11	3.5 × 3.5	EC	n	dusty core shocks impressive
Camargo 333	275.142	-0.77	9 : 31 : 31	−52 : 30 : 17	10 × 10	EGr	y	impressive winds
Camargo 334	275.14	-1.07	9 : 30 : 09	−52 : 43 : 35	7 × 7	ECC	n	
Camargo 335	275.17	-0.98	9 : 30 : 40	−52 : 40 : 49	7 × 7	EC	y	small core
Camargo 336	275.57	-2.20	9 : 26 : 58	−53 : 50 : 13	5 × 5	EC	y	
Camargo 337	275.65	-2.19	9 : 27 : 27	−53 : 53 : 04	6 × 6	EC	n	winds
Camargo 338	275.71	-2.31	9 : 27 : 11	−54 : 00 : 43	6 × 6	EGr	n	winds
Camargo 339	275.72	-2.23	9 : 27 : 35	−53 : 57 : 34	10 × 10	EC	n	cavity, winds
Camargo 340	275.80	-2.20	9 : 28 : 08	−53 : 59 : 51	7 × 7	EC	n	impressive
Camargo 341	275.88	-2.15	9 : 28 : 45	−54 : 00 : 50	7 × 7	EGr	n	
Camargo 342	275.97	-2.03	9 : 29 : 46	−53 : 59 : 22	8 × 8	EC	n	prominent
Camargo 343	276.01	-1.79	9 : 31 : 05	−53 : 50 : 23	7 × 7	EC	y	impressive, dusty core
Camargo 344	276.03	-1.45	9 : 32 : 43	−53 : 36 : 21	3 × 3	EC	n	include subcluster
Camargo 345	276.04	-1.00	9 : 34 : 51	−53 : 17 : 11	9 × 9	EC	n	winds impressive

Table A.4 (continued)

Target	ℓ	b	α(2000)	δ(2000)	Size	Type	Avend.	Comments
	(°)	(°)	(h m s)	(° ′ ″)	(′)			
(1)	(2)	(3)	(4)	(5)	(6)	(7)	(8)	(9)
Camargo 346	276.07	-1.44	9 : 33 : 02	−53 : 37 : 36	9 × 9	EC	n	incl. subcl. cavity
Camargo 347	276.38	-2.64	9 : 28 : 58	−54 : 42 : 56	5 × 5	EC	n	object is a loose core?
Camargo 348	276.51	-2.45	9 : 30 : 29	−54 : 40 : 14	7 × 7	EC	n	dusty core
Camargo 349	276.58	-3.88	9 : 23 : 54	−55 : 44 : 35	8 × 8	EGr	n	
Camargo 350	276.60	-1.91	9 : 33 : 27	−54 : 20 : 01	6 × 6	EC	n	impressive
Camargo 351	276.61	-1.72	9 : 34 : 24	−54 : 12 : 08	7 × 7	EGr	n	
Camargo 352	276.70	-1.47	9 : 36 : 00	−54 : 04 : 35	8 × 5	EGr	n	
Camargo 353	276.74	-1.60	9 : 35 : 39	−54 : 11 : 40	8 × 8	EC	n	
Camargo 354	276.97	-4.02	9 : 25 : 10	−56 : 06 : 45	6 × 6	EC	n	prominent
Camargo 355	277.06	-3.16	9 : 29 : 54	−55 : 33 : 19	9 × 9	EC	n	
Camargo 356	277.13	-1.53	9 : 37 : 58	−54 : 24 : 25	5 × 5	EGr	n	
Camargo 357	277.15	-1.60	9 : 37 : 42	−54 : 28 : 04	7 × 7	EC	n	prominent
Camargo 358	277.22	-1.55	9 : 38 : 18	−54 : 28 : 42	6 × 6	EC	n	prominent
Camargo 359	277.23	0.64	9 : 48 : 00	−52 : 49 : 47	9 × 9	EC	n	core, prominent
Camargo 360	277.36	-1.36	9 : 39 : 56	−54 : 25 : 46	8 × 8	EC	n	prominent
Camargo 361	277.50	-1.23	9 : 41 : 13	−54 : 25 : 23	7 × 6	EGr	n	1st generation, bubble
Camargo 362	277.51	-1.28	9 : 41 : 02	−54 : 28 : 18	6 × 6	EGr	n	protocl, 2nd gener winds, dusty core
Camargo 363	277.52	-3.32	9 : 31 : 28	−55 : 59 : 33	8 × 8	EGr	n	
Camargo 364	277.56	0.56	9 : 49 : 19	−53 : 05 : 43	8 × 8	EGr	n	
Camargo 365	277.63	-1.05	9 : 42 : 42	−54 : 22 : 25	6 × 6	EC	y	dusty core
Camargo 366	277.68	0.89	9 : 51 : 20	−52 : 54 : 49	9 × 9	EGr	n	
Camargo 367	277.69	-3.15	9 : 33 : 10	−55 : 58 : 52	10 × 10	EGr	n	
Camargo 368	277.71	0.51	9 : 49 : 54	−53 : 13 : 48	10 × 10	EGr	n	winds
Camargo 369	277.80	0.50	9 : 50 : 18	−53 : 17 : 38	6 × 6	EC	n	bubble, winds, impressive
Camargo 370	277.84	-3.08	9 : 34 : 20	−56 : 01 : 30	8 × 8	EC	n	impressive
Camargo 371	277.94	-1.43	9 : 42 : 34	−54 : 51 : 48	6 × 6	EGr	n	protocl, winds, dusty core
Camargo 372	277.95	-2.65	9 : 36 : 58	−55 : 47 : 20	8 × 8	EGr	n	
Camargo 373	278.35	-0.89	9 : 47 : 09	−54 : 43 : 10	8 × 8	EC	y	impressive, dusty core
Camargo 374	278.60	-0.99	9 : 48 : 02	−54 : 57 : 18	8 × 8	EC	n	loose core
Camargo 375	278.63	-0.37	9 : 50 : 56	−54 : 29 : 41	6 × 6	EC	y	impressive stellar and dusty core
Camargo 376	278.78	-0.65	9 : 50 : 31	−54 : 48 : 25	6 × 6	EC	n	protocl., bubble, winds
Camargo 377	279.04	-1.13	9 : 49 : 49	−55 : 20 : 45	7 × 7	EC	n	
Camargo 378	279.12	-1.22	9 : 49 : 52	−55 : 27 : 39	6 × 6	EGr	n	
Camargo 379	279.12	-1.22	9 : 49 : 32	−55 : 50 : 07	10 × 10	EGr	n	
Camargo 380	279.40	-1.68	9 : 49 : 19	−55 : 59 : 45	3 × 2	EC	n	2nd generation, deeply absorbed
Camargo 381	279.42	-0.96	9 : 52 : 39	−55 : 27 : 10	6 × 6	EGr	y	bubble, impress, 1st and 2nd gener
Camargo 382	279.43	-1.69	9 : 49 : 17	−56 : 02 : 27	5 × 5	EC	n	1st generation, shock,core
Camargo 383	279.50	-1.52	9 : 50 : 35	−55 : 56 : 17	7 × 7	EC	n	
Camargo 384	279.52	-1.73	9 : 49 : 44	−56 : 06 : 48	6 × 6	EC	n	core
Camargo 385	279.57	-1.42	9 : 51 : 27	−55 : 54 : 12	6 × 6	EC	y	
Camargo 386	279.67	-1.02	9 : 53 : 47	−55 : 39 : 02	5 × 5	EGr	n	prominent
Camargo 387	279.93	-0.40	9 : 57 : 56	−55 : 19 : 49	11 × 11	EGr	n	
Camargo 388	280.00	-1.20	9 : 54 : 47	−55 : 59 : 49	6 × 6	EC	n	winds, impressive
Camargo 389	280.02	-1.42	9 : 53 : 57	−56 : 10 : 56	7 × 7	EC	n	impressive, core
Camargo 390	280.37	-1.68	9 : 54 : 46	−56 : 36 : 20	8 × 8	EGr	n	winds
Camargo 391	280.43	-1.23	9 : 57 : 09	−56 : 17 : 09	7 × 7	EC	n	poor core
Camargo 392	280.43	-1.74	9 : 54 : 48	−56 : 41 : 15	8 × 8	EC	n	small core, winds,impressive
Camargo 393	280.44	-1.83	9 : 54 : 30	−56 : 45 : 46	7 × 7	EGr	n	winds
Camargo 394	280.46	-1.02	9 : 58 : 12	−56 : 08 : 24	6 × 6	EC	n	
Camargo 395	280.51	-0.99	9 : 58 : 38	−56 : 08 : 48	6 × 6	EC	n	dusty core
Camargo 396	280.57	-0.47	10 : 01 : 11	−55 : 46 : 01	6 × 6	EC	n	loose core
Camargo 397	280.58	-1.44	9 : 57 : 02	−56 : 32 : 23	8 × 8	EGr	n	cavities
Camargo 398	280.62	-1.19	9 : 58 : 22	−56 : 22 : 13	6 × 6	EC	y	prominent, dusty core
Camargo 399	280.65	-1.27	9 : 58 : 12	−56 : 27 : 03	7 × 7	EC	y	impressive, central concentration
Camargo 400	280.66	-0.88	9 : 59 : 56	−56 : 09 : 03	6 × 6	EC	n	impressive
Camargo 401	280.69	-1.15	9 : 58 : 58	−56 : 22 : 58	6 × 6	EGr	n	
Camargo 402	280.76	-1.33	9 : 58 : 34	−56 : 34 : 13	10 × 10	EC	y	dusty core
Camargo 403	280.78	-1.06	9 : 59 : 50	−56 : 21 : 58	7 × 5	EC	n	dusty core
Camargo 404	280.89	-0.55	10 : 02 : 41	−56 : 01 : 30	7 × 7	EGr	n	bubble
Camargo 405	280.99	-1.53	9 : 59 : 00	−56 : 51 : 42	6 × 6	EC	y	wind,impressive
Camargo 406	281.05	-1.55	9 : 59 : 15	−56 : 54 : 46	6 × 6	EC	y	dusty core
Camargo 407	281.06	-1.73	9 : 58 : 29	−57 : 04 : 15	5 × 5	EC	n	core
Camargo 408	281.08	-2.55	9 : 54 : 53	−57 : 43 : 36	9 × 9	EGr	n	inc. promin 9 sharp edge dust neb
Camargo 409	281.09	-1.59	9 : 59 : 17	−56 : 58 : 39	4 × 4	EC	y	protocluster? impressive, rel DBS 125
Camargo 410	281.12	-1.15	10 : 01 : 26	−56 : 38 : 49	7 × 7	EGr	n	cavity
Camargo 411	281.22	-1.26	10 : 01 : 33	−56 : 47 : 15	7 × 7	EC	y	compact core, stellar and dusty
Camargo 412	281.26	-1.69	9 : 59 : 52	−57 : 09 : 29	6 × 6	EC	y	core
Camargo 413	281.30	-2.25	9 : 57 : 32	−57 : 37 : 38	6 × 6	EC	n	loose poor core
Camargo 414	281.42	-1.80	10 : 00 : 18	−57 : 20 : 34	12 × 12	EC	n	inc. subclusters, 2nd gener, impres

Table A.4 (continued)

Target	ℓ	b	α(2000)	δ(2000)	Size	Type	Avend.	Comments
	(°)	(°)	(h m s)	(° ′ ″)	(′)			
(1)	(2)	(3)	(4)	(5)	(6)	(7)	(8)	(9)
Camargo 415	281.50	-2.55	9 : 57 : 23	−57 : 59 : 20	6 × 6	EC	y	core, impressive
Camargo 416	281.53	-1.82	10 : 00 : 54	−57 : 25 : 49	7 × 7	EC	n	winds, impressive core
Camargo 417	281.56	-2.48	9 : 58 : 02	−57 : 50 : 00	6 × 6	EC	n	dusty core, impressive
Camargo 418	281.63	-1.29	10 : 03 : 49	−57 : 03 : 57	7 × 7	EC	n	poor core
Camargo 419	281.64	-2.54	9 : 58 : 14	−58 : 04 : 06	8 × 8	EC	n	core, prominent
Camargo 420	281.65	-2.07	10 : 00 : 28	−57 : 41 : 57	4 × 4	ECC	n	protocl? bubble, core, dust & 3 sts
Camargo 421	281.69	-2.06	10 : 00 : 44	−57 : 42 : 48	6 × 6	EC	y	core, impressive
Camargo 422	281.70	-1.10	10 : 05 : 05	−56 : 57 : 02	6 × 6	EC	y	small dusty core
Camargo 423	281.81	-1.09	10 : 05 : 46	−57 : 00 : 16	6 × 6	EC	n	poor core, impressive
Camargo 424	281.86	-1.65	10 : 03 : 37	−57 : 29 : 24	2 × 2	EC	y	dusty core
Camargo 425	281.87	-2.12	10 : 01 : 33	−57 : 51 : 59	7 × 7	EGr	y	wind very poor core?
Camargo 426	281.88	-1.85	10 : 02 : 49	−57 : 39 : 50	7 × 7	EC	n	impressive, core
Camargo 427	281.94	-1.52	10 : 04 : 36	−57 : 25 : 52	7 × 7	EC	n	small dusty core
Camargo 428	281.98	-1.37	10 : 05 : 32	−57 : 19 : 48	6 × 6	EC	y	small dusty core, prominent
Camargo 429	282.00	-1.72	10 : 04 : 07	−57 : 37 : 50	8 × 8	EGr	n	winds, impressive
Camargo 430	282.05	-1.41	10 : 05 : 48	−57 : 24 : 21	5 × 5	EC	n	small impressive core
Camargo 431	282.06	-1.85	10 : 03 : 55	−57 : 46 : 09	6 × 6	EC	y	small dusty core, winds
Camargo 432	282.06	-2.12	10 : 02 : 44	−57 : 58 : 51	7 × 7	EC	n	poor core, prominent, bubble
Camargo 433	282.16	-1.57	10 : 05 : 47	−57 : 35 : 51	6 × 6	EC	n	loose dusty core
Camargo 434	282.22	-2.13	10 : 03 : 36	−58 : 05 : 04	6 × 6	EC	n	small dusty core
Camargo 435	282.35	-1.85	10 : 05 : 42	−57 : 56 : 11	6 × 6	EC	n	unique long core, impressive
Camargo 436	282.52	-1.98	10 : 06 : 07	−58 : 08 : 11	6 × 6	EC	n	loose core, impressive
Camargo 437	289.29	-3.93	10 : 44 : 38	−63 : 23 : 22	5 × 5	EC	n	complex core struct in W3 and W4

Note. — Cols. 2 – 5: Central coordinates. Col. 6: cluster size. Col. 7: object type - OC means open cluster, OCC open cluster candidate, EC embedded cluster, ECC embedded cluster candidate, EGr stellar group, and SFN star-forming nebulae. Col. 8: cross-identifications with Avedisova (2002) SFRs or candidates within 5' of the central coordinates, y and n means yes and not.